Continental Shelf Research 30 (2010) 1924–1940

Contents lists available at ScienceDirect

Continental Shelf Research

journal homepage: www.elsevier.com/locate/csr

Research papers

Tracing the influence of sewage discharge on coastal bays of Southern Vancouver Island (BC, Canada) using sedimentary records of phytoplankton

Alanna Krepakevich*, Vera Pospelova

School of Earth and Ocean Sciences, University of Victoria, Bob Wright Centre A405, PO Box 3065 STN CSC, Victoria, BC, Canada V8W 3V6

A R T I C L E I N F O

Article history:
Received 8 April 2010
Received in revised form
19 August 2010
Accepted 1 September 2010
Available online 9 September 2010

Keywords:
Eutrophication
Dinoflagellate cysts
Toxic species
Sewage
Estuaries
British Columbia

A B S T R A C T

The impact of sewage and stormwater effluents on phytoplankton is investigated by comparing organic-walled dinoflagellate cyst abundance and diversity from 38 surface sediment samples, flanking southern Vancouver Island. Site locations include those directly adjacent to wastewater outfall at Clover and Macaulay Points and Saanich Peninsula, as well as from a variety of near-shore environments with differing tidal flow influences. Excellently preserved dinoflagellate cyst assemblages have been recovered and 36 cyst taxa were identified. Local assemblages are characterized by a high relative proportion (average 56%) of cysts produced by heterotrophic dinoflagellates, which is typical for regions of high primary production. Relative proportional increases of cysts from heterotrophic species with particular increases of *Polykrikos kofoidii/schwartzii* and *Dubridinium* species, known to reflect areas affected by eutrophication, occur directly adjacent to all three sewage outfalls, as well as in the more stagnant waters of Esquimalt and Victoria Harbours and at the mouth of Cadboro Bay. Further effects of an anthropogenic effluent can be seen in the relatively higher concentrations of organic carbon and the diatom production proxy, biogenic opal. Results from this study clearly indicate a much larger impact zone than predicted by a sewage effluent plume model or trends found in monitored benthic biota and sediment chemistry that evidence primary outfall affects <800 m eastward of Macaulay Point and about 200 m eastward of the Clover Point. Enhanced production of cysts from potentially toxic *Alexandrium* species is also observed near locations of sewage outfalls.

1. Introduction

Concern about human-induced coastal eutrophication has prompted a search for biological indicators that can be used to assess present and past status of an estuarine health. Understanding what impact that an anthropogenic effluent has on urbanized coastal waters and environs is critical to sustainable marine management. Cultural eutrophication, the process by which nutrient or organic matter supply to coastal waters is increased due to human activities, results in changes to the ecosystem that include enhanced primary production and assemblage variation that may radiate through upper trophic levels, as well as possible bottom water hypoxia or anoxia (Nixon, 1995). There is cause for even greater concern when eutrophication causes blooms of toxic phytoplankton species near urbanized centers.

Dinoflagellates are extremely diverse and complex single-celled protists that comprise a significant proportion of coastal planktonic biomass in their biflagellate motile stage. As part of their life cycle, numerous species produce a very resistant, organic-walled benthic resting cyst that is typically well preserved in the sedimentary record (Dale, 1976; Taylor, 1987; Fensome et al., 1993). While approximately half of cyst-producing dinoflagellate species are heterotrophic, the remainder are phototrophic and/or mixotrophic (Dale, 2009). Sedimentary records from coastal sites may represent 30–40% of the dinoflagellate species included in the resident plankton population (Dale, 2009). Dinoflagellate cysts are accepted as biological indicators in paleoenvironmental reconstructions, since their assemblage is known to reflect environmental parameters through a direct correlation with physical changes in sea surface conditions, such as water temperature, salinity, light and nutrient availability (e.g. Taylor, 1987; Dale, 1996, 2009; Dale et al., 1999; Rochon et al., 1999; Matsuoka, 1999; de Vernal et al., 2001, 2005; Pospelova et al., 2004; Radi and de Vernal, 2004; Radi et al., 2007; Pospelova et al., 2008). Increased proportions of heterotrophic taxa (particularly Protoperidinoids) are typical in coastal upwelling zones as increased nutrient availability likely increases production of their prey (e.g. Wall et al., 1977; Lewis et al., 1990; Dale, 1996; Harland et al., 1998; Zonneveld et al., 2001; Dale et al., 2002; Marret and Zonneveld, 2003; Reichart and Brinkhuis, 2003;

* Corresponding author.
E-mail addresses: alanna.jane@yahoo.ca (A. Krepakevich), vpospe@uvic.ca (V. Pospelova).

0278-4343/$ - see front matter © 2010 Elsevier Ltd. All rights reserved.
doi:10.1016/j.csr.2010.09.002

Radi and de Vernal, 2004; Pospelova et al., 2006, 2008; Thibodeau et al., 2006; Holzwarth et al., 2007, 2010; Marret et al., 2008; González et al., 2008; Bouimetarhan et al., 2009). Commonly, areas affected by cultural eutrophication are characterized by high heterotrophic fractions combined with an express increase in cysts of Polykrikaceae and Diplopsalidaceae dinoflagellates, specifically those of Polykrikos kofoidii/schwartzii and Dubridinium species (Matsuoka, 1999; Pospelova et al., 2002; Matsuoka et al., 2003; Pospelova et al., 2005; Ellegaard et al., 2006; Dale, 2009). Alternative signals attributed to eutrophication, in particular the increase of Lingulodinium machaerophorum, have also been linked to select locations (Thorsen and Dale, 1997; Dale et al., 1999). It was later argued that the latter signal might manifest in deep stratified waters, and not be present in shallower well-mixed environments (Pospelova et al., 2002).

The purpose of this paper is to investigate the patterns of dinoflagellate cyst distribution along the urbanized coast of the Capital Regional District (CRD), Southern Vancouver Island. We use the sedimentary record of dinoflagellate cysts and the diatomaceous proxy biogenic silica at a very high spatial scale, in order to elucidate the possible response of local phytoplankton to current wastewater management practices in this region. Since July 2006 British Columbia Minister of the Environment directive obliging the CRD to extend into secondary sewage treatment (CRD, 2008b; Chapman, 2006), the treatment plant initiative has been underway. Secondary treatment would not necessarily remove nutrients (nitrogen and phosphorus) responsible for an eutrophication (Stubblefield et al., 2006), thus affecting the phytoplankton community in the receiving environment. While this study addresses the current status of the phytoplankton community along the CRD coast, it also sets an important reference point for the future. Forthcoming studies of the phytoplankton community can then be contrasted with the current study, in order to extract an unambiguous signal of nutrient enrichment imprinted in the phytoplankton sedimentary record.

2. Regional setting

The City of Victoria and surrounding CRD are located on the southeastern tip of Vancouver Island on the Canadian west coast (Fig. 1). Local hydrology is largely governed by an estuarine flow through Juan de Fuca Strait, as well as by strong tidal currents that are influenced by the highly variable coastline (Mackas and Harrison, 1997; Thomson et al., 2007). As the principal link

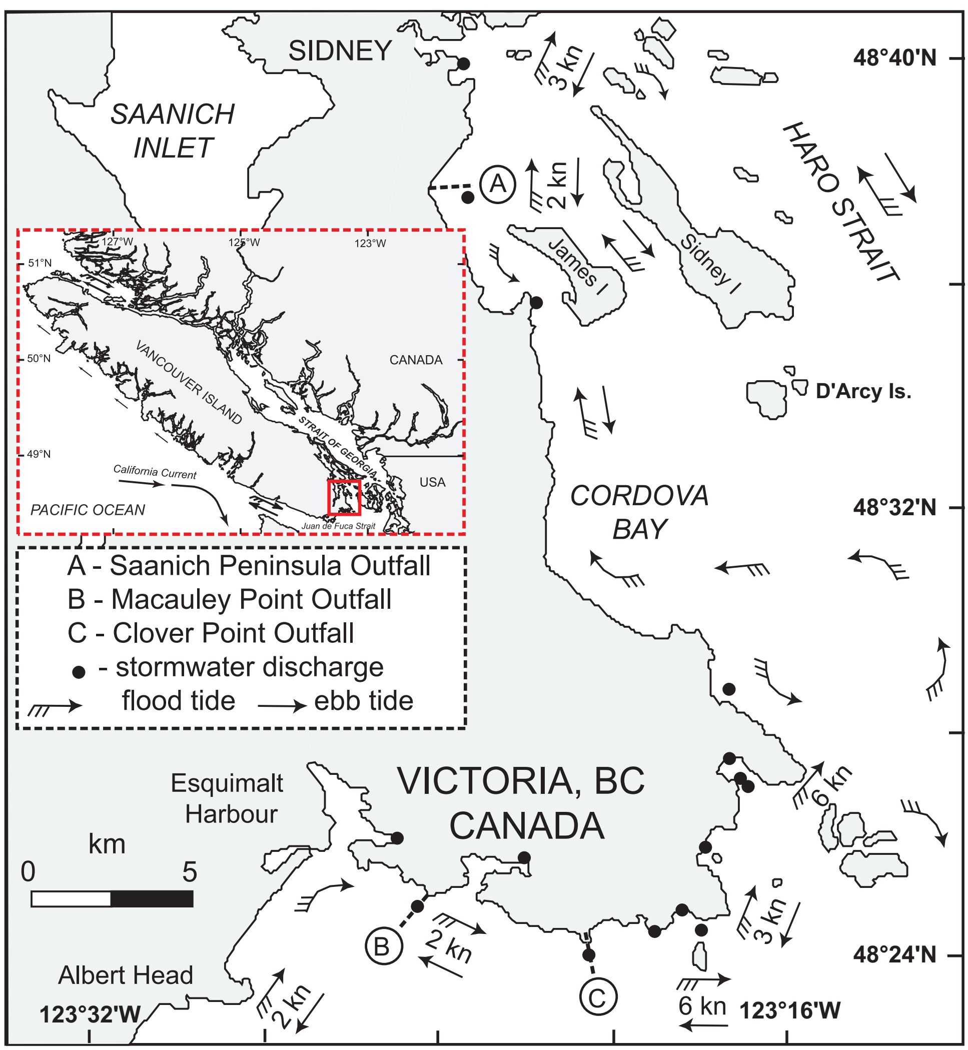

Fig. 1. Map showing geographical locations of Southern Vancouver Island sewage outfall (dashed lines) and stormwater discharge stations (black dots) and a schematic representation of effective tidal currents that act on the effluent plume (compiled from Foreman et al., 1995; Stubblefield et al., 2006; Radi et al., 2007; Thomson et al., 2007, and an online Government of Canada Department of Fisheries and Oceans tidal model that can be found at http://www-sci.pac.dfo-mpo.gc.ca/juandefuca/modelnew_e.asp).

between the Pacific Ocean and inner Strait of Georgia, Juan de Fuca Strait is fed by deep, nutrient-rich shoreward flow enhanced by offshore upwelling and a surface, seaward flow driven predominantly by Fraser River runoff from the mainland. Conversely, estuarine circulation is not entirely constant in this region. Thomson et al. (2007) use the results from 7-year current measurement program across mid-channel Juan de Fuca Strait to illustrate that the system undergoes a flow regime shift, during episodes of poleward coastal wind, from estuarine (net outflow) to transient (net inflow) that persists for days in the summer and up to weeks in the winter. Estuarine flow is also hindered on a fortnightly tidal cycle, whereby intensified mixing above the Victoria and Boundary Pass sills during spring tides creates a hydraulic barrier that inhibits surface seaward flow and subsequent deep return (Thomson et al., 2007) and by large-scale turbulent eddies created as tidal flow contacts the irregular coastline (Chandler and Gormican, 2001). Additionally, the area directly offshore the city of Victoria is a degenerate semi-diurnal amphidrome, thus only affected by the tidal range attributed to the diurnal cycle (Thomson et al., 2007; Foreman et al., 1995). Despite the complex hydrology, the entire Georgia Basin is rapidly flushed (average residence time 1 year), and waters typically remain weakly stratified since local bathymetry, wind and tides promote vertical mixing (Mackas and Harrison, 1997). Within the study area, surface water property values vary little. Mean surface salinity remains nearly constant throughout the year, while mean surface temperature values range between about 7 °C in February and just over 12 °C in August (Table 1). There is no seasonal ice cover in this region.

Within this complex physical environment, two submerged outfall systems release raw sewage into coastal waters, adjacent to Victoria. After preliminary screening for solids larger than 6 mm, discharge occurs at depths of 60 m, 1.8 km offshore at Macaulay Point and at 67 m, 1.1 km offshore at Clover Point (Fig. 2) (CRD, 2000, 2008b). Macaulay Point is characterized as a lower energy environment depositing medium sand to silt, while the much greater tidal exchange at Clover Point drives rapid currents that deposit coarser-grained sediments (Fig. 1, Table 1). An additional outfall station discharges secondary treated wastewater from a multi-port outfall at 30 m depth, about 1.6 km off Saanich Peninsula, into Bazan Bay (Fig. 2) (CRD, 2007, 2008a). The 2007 total nitrogen loadings from these three main CRD outfalls were 1441.7 tonnes N/yr (Macaulay Point: 751, Clover Point: 659, Saanich Peninsula: 31.7 tonnes N/yr) or about 3.96 tonnes N/d (Macaulay Point: 2.06, Clover Point: 1.81, Saanich Peninsula: 0.09 tonnes N/d) (personal correspondence: Taylor, CRD Senior Manager Scientific Program). These values comprise the contribution from nitrate, nitrite, and total Kjeldahl nitrogen (including ammonia/ammonium and organic nitrogen). A nested 3D model of local plume dispersion predicts the most frequent neutral buoyancy trapping depth to be 45 m at Macaulay Point and 50–55 m

Table 1
Coordinates, water depth and sedimentary type of samples used in this study, together with average surface water salinity and temperature for February and August. Surface water property values are taken from the World Ocean Atlas 2001 CD-ROM (WOA01) of the National Oceanographic Data Center (NODC, 1994; http://www.nodc.noaa.gov/OC5/WOA01/pr_woa01.html). Boyer et al., (2002), Conkright et al., (2002) and Stephens et al., (2002) review the statistical treatment of that dataset.

Sample ID	Coring device	Latitude (°N)	Longitude (°W)	Water depth (m)	Sediment type	Temperature February (°C)	Temperature August (°C)	Salinity February	Salinity August
1	Box	48.3871	−123.4702	40	Coarse sand	7.11	11.98	29.25	29.73
3	Gravity	48.4136	−123.4730	22	Fine sand to silt	7.09	12.00	29.17	29.67
5	Gravity	48.4486	−123.4430	8	Fine sand to silt	7.08	12.02	29.15	29.54
6	Gravity	48.4423	−123.4441	11	Fine sand to silt	7.09	12.02	29.17	29.57
7	Gravity	48.4308	−123.4434	16	Fine sand to silt	7.09	12.02	29.17	29.57
8	Gravity	48.4135	−123.4389	52	Medium sand to silt	7.03	12.02	29.24	29.64
10	Box	48.3953	−123.4042	62	Coarse sand to silt	7.04	12.06	29.24	29.60
11	Box	48.4010	−123.3990	70	Coarse sand to silt	7.04	12.08	29.24	29.58
14	Box	48.3993	−123.4205	57	Medium sand to silt	7.05	12.05	29.25	29.61
16	Box	48.4053	−123.3896	65	Medium sand to silt	7.04	12.08	29.23	29.58
17	Box	48.4097	−123.4235	50	Medium sand to silt	7.04	12.05	29.22	29.61
18	Box	48.4104	−123.4108	55	Medium sand to silt	7.03	12.08	29.22	29.57
19	Box	48.4162	−123.4049	15	Medium sand to silt	7.02	12.08	29.20	29.55
20	Box	48.4021	−123.3588	17	Coarse sand	7.05	12.11	29.23	29.57
22	Box	48.4009	−123.3453	30	Coarse sand	7.04	12.13	29.20	29.54
23	Box	48.4060	−123.3407	11	Coarse sand	7.04	12.13	29.19	29.54
24	Box	48.3983	−123.3439	40	Coarse sand	7.05	12.12	29.20	29.55
26	Box	48.3946	−123.3478	64	Coarse sand	7.05	12.11	29.20	29.56
28	Box	48.3895	−123.3468	100	Coarse sand	7.05	12.11	29.23	29.57
29	Box	48.4184	−123.3923	11	Fine sand to silt	7.02	12.08	29.20	29.49
30	Gravity	48.4275	−123.3958	4	Fine sand to silt	7.02	12.08	29.20	29.47
31	Box	48.4337	−123.2978	10	Medium sand to silt	7.03	12.18	29.01	29.32
33	Gravity	48.4551	−123.2919	8	Fine sand to silt	7.00	12.21	28.97	29.25
34	Gravity	48.4504	−123.2870	9	Fine sand to silt	7.01	12.19	28.99	29.29
35	Gravity	48.4402	−123.2757	20	Fine sand to silt	7.02	12.20	28.98	29.24
37	Gravity	48.4680	−123.2840	12	Fine sand to silt	7.00	12.24	28.95	29.08
39	Box	48.4778	−123.2804	36	Coarse sand to silt	6.99	12.24	28.96	29.03
40	Gravity	48.4753	−123.2963	12	Fine sand to silt	6.99	12.23	28.99	29.09
43	Box	48.4950	−123.3186	6	Medium sand to silt	7.00	12.20	29.05	29.20
44	Box	48.5070	−123.3415	10	Fine sand to silt	6.99	12.22	29.06	29.18
49	Box	48.6279	−123.3964	15	Fine sand to silt	6.94	12.29	28.81	27.77
50	Box	48.6287	−123.3850	29	Coarse sand	6.94	12.29	28.80	27.77
52	Box	48.6335	−123.3836	19	Coarse sand	6.93	12.29	28.79	27.73
54	Box	48.6504	−123.3784	32	Coarse sand	6.97	12.31	28.69	27.66
55	Box	48.6491	−123.3171	46	Gravel to coarse sand	6.96	12.36	28.64	27.60
58	Box	48.6713	−123.4027	8	Fine sand to silt	6.96	12.34	28.66	27.54
59	Box	48.6725	−123.4105	4	Medium sand to silt	6.97	12.34	28.66	27.54
60	Box	48.5960	−123.3801	9	Medium sand to silt	6.96	12.27	28.91	28.65

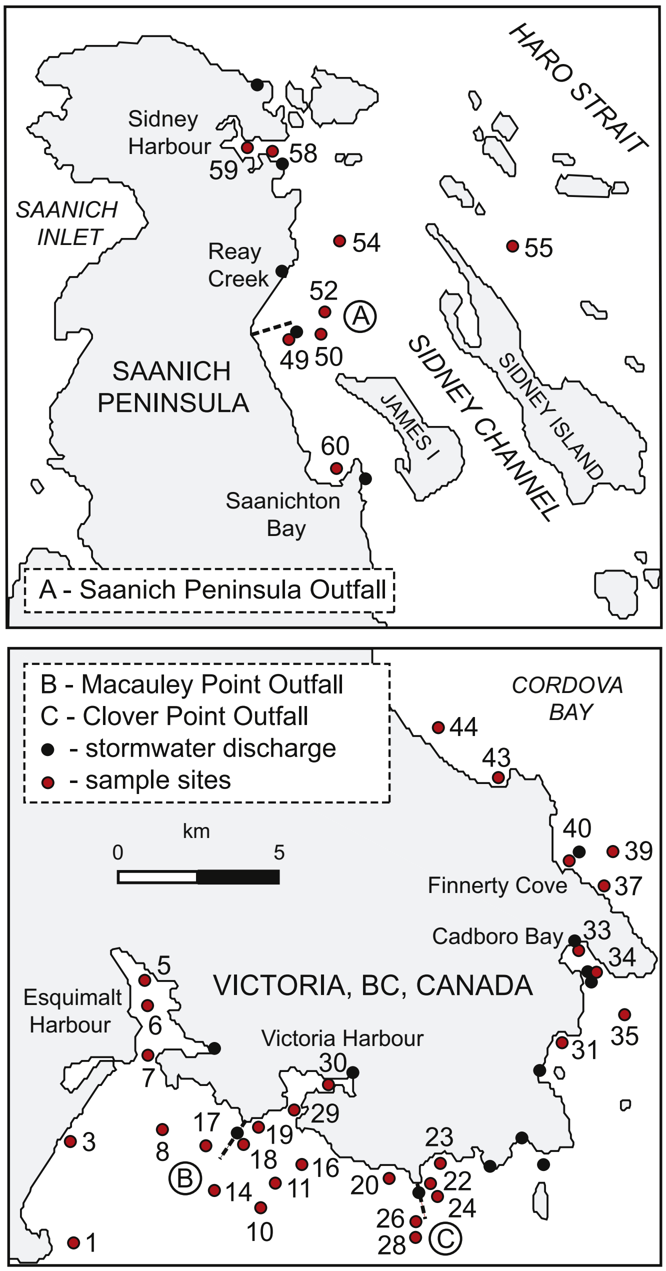

Fig. 2. Map of study area showing sample site locations in relation to the three sewage outfall stations, planned stormwater discharge sites and various coastal features.

at Clover Point, with dilution factors ranging 410:1–720:1 the majority of the time (Hodgins et al., 1998: Hodgins, 2006). Stormwater, combined with wastewater overflow, is also discharged periodically from at least 16 outfalls within the study area (Fig. 2) (CRD, 2000, 2008c). Overflow release into these sites primarily occur during significant storm events or power outages (CRD, 2000), yet unlike regular outfall, discharge takes place within the surface waters rather than into deeper inflow waters naturally rich in nutrients from offshore upwelling. For example, planned stormwater discharge destinations include Portage Inlet and the Gorge waterway that empty into Victoria Harbour, Lang Cove in Esquimalt Harbour, 307 m offshore of Macaulay Point (discharging to 11 m depth), 340 and 80 m offshore of Clover Point (13 and 5 m depth, respectively), 110 and 220 m into the mouth of Cadboro Bay discharging particles smaller than 12 mm (at depths of 7.2 and 3.8 m, respectively) with an additional storm drain at Gyro Beach Park within Cadboro Bay, 400 m offshore of Finnerty Cove (14 m depth), Tsawout First Nation sewage outfall near Saanichton Bay, North Saanich Marina outfall at the mouth of Sidney Harbour and Reay Creek, which discharges near the Saanich Peninsula Outfall, drains both the airport area and Sidney (Fig. 2) (CRD, 2000, 2008c).

A robust assessment of the Juan de Fuca Strait/Georgia Basin system for an eutrophication potential denotes that despite natural input of nutrients from offshore upwelling greatly exceeding those from anthropogenic sources, high average ambient nitrogenous concentrations (2–20 μM N) and dispersal by strong tidal currents, the basin topography may allow for localized cultural eutrophication in more isolated bays with low flushing rates (Mackas and Harrison, 1997). 'Reversed' transient flow driven by downwelling favorable winds also enhances the likelihood of retaining both anthropogenic effluent and natural nutrient input within the system due to a net landward flow (Thomson et al., 2007).

3. Materials and methods

3.1. Sediment collection and laboratory treatments

The sediment samples used in this study were collected from the upper two centimeters of core-tops obtained with a light gravity or box corer on research cruises September 26/27, 2007 (sites 1–44) and July 02, 2008 (sites 46–60) (Fig. 2). Sample 30 from Victoria Harbour was obtained in September 2007 by light gravity corer. Geographical coordinates and sediment type of all sites are recorded in Table 1, along with water depth, average February and August sea surface salinity and temperature. Sediment type corresponds to an actual grain size determined at the Bedford Institute of Oceanography Sedimentary Laboratory in Dartmouth, Nova Scotia by laser analysis with a Beckman Coulter LS230 analyzer after removing organics with 35% hydrogen peroxide, sieving to separate <63 μm, $>63/<2000$ μm, >2000 μm fractions and freeze drying. Surface water salinity and temperature values originate from the World Ocean Atlas 2001 CD-ROM (WOA01) of the National Oceanographic Data Center (NODC, 1994; http://www.nodc.noaa.gov/OC5/WOA01/pr_woa01.html). Boyer et al. (2002), Conkright et al. (2002) and Stephens et al. (2002) review the statistical treatment of that dataset. Based on ^{210}Pb supported sediment accumulation rates in the greater Strait of Georgia and Puget Sound areas, each sample provides an integrated record of approximately the last 1–4 years (Lavelle et al., 1986; Johannessen et al., 2003).

Recovery of organic-walled dinoflagellate cysts (dinocysts) was achieved by following a standard palynological processing technique (Pospelova et al., 2005). Sub-samples of the known volume were initially oven-dried at 40 °C and weighed analytically. One tablet of exotic marker grains of *Lycopodium clavatum* spores (Batch no. 483216) was added to each sample for the subsequent determination of absolute dinocyst abundance (Stockmarr, 1977). Samples were first treated with 10% hydrochloric acid (HCl) at room temperature for the removal of carbonate phases, rinsed twice with distilled water and sieved through 120-μm and retained on 15-μm mesh, in order to eliminate both coarse and very fine fractions. Siliceous phases were digested by the addition of 49% hydrofluoric acid (HF) at room temperature for up to four days. Any precipitation of calcium fluoride was then removed with cold 10% hydrochloric acid for a total HCl exposure of 20 min maximum per sample. After each stage, the sample was rinsed with distilled water and centrifuged. In order to avoid damaging or destroying more delicate dinoflagellate cysts, oxidizing agents were avoided throughout the procedure (Dale, 1976; Zonneveld et al., 1997; Versteegh and Zonneveld, 2002; Zonneveld et al., 2007, 2008). The organic residue was finally rinsed twice with distilled water, sonicated for up to 1 min and collected on a 15-μm mesh. Aliquots of the residue were slide mounted in glycerine jelly on a low temperature hotplate. Dinocysts were identified and counted, using the Nikon Eclipse 80i transmitted light microscope at 600–1000 × magnifications (Plates 1–3). An average of ∼200 dinoflagellate cysts was counted in 35 of the surface samples, with a maximum of 570 cysts. Although the remaining three samples were counted and are included in the overall survey, their cyst concentrations of 28 (site 17), 32 (site 23) and 42 (site 59) are considered too sparse to be included in the statistical analysis.

Additional sub-samples were freeze dried at −80 °C and powdered in preparation for geochemical analysis. Proportions of total carbon (TC) and total nitrogen (N) were determined for sub-samples of the known weight by high-temperature flash combustion using the Fisons NA 1500 elemental analyzer, after calibration by PACS sediment standards (Verado et al., 1990). Inorganic carbon (IC) content of sediment samples was determined at the University of British Columbia (UBC) Inorganic Geochemical Laboratory, after an acid evolution of carbon dioxide, using UIC Inc. CM5014 CO_2 coulometer. Weight % IC values were then employed to determine organic carbon content by subtraction from total carbon percents (OC=TC–IC). Biogenic opal fractions were also ascertained at the UBC Inorganic Geochemical Laboratory, using the standard wet-alkaline procedure that digests carbonate and organic phases, subjects opal surfaces to dissolution, and then analyzes the supernatant by molybdate-blue spectrophotometry (Mortlock and Froelich, 1989). As this procedure is known to dissolve very little inorganic silica at the end of 5 h in 2 M Na_2CO_3, marginal error occurs by overestimation of opal from inorganic fractions. Most diatomaceous silica younger than 30 million years typically contains an approximately constant water content of 10%, therefore weight percent biogenic opal is taken to be $\%OPAL = 2.4 \times \%Si_{OPAL}$ (Mortlock and Froelich, 1989).

3.2. Dinoflagellate cyst nomenclature

Dinoflagellate cyst taxonomical nomenclature used is in accordance with the established database given in Lentin and Williams (1993) and subsequent taxonomic descriptions found in Head (1996), Zonneveld (1997), Rochon et al. (1999), Head et al. (2001), Head (2002), Pospelova and Head (2002), Kawami et al. (2009) and Matsuoka et al. (2009). This paleontological taxonomy of dinoflagellate cysts differs from the biological taxonomy of motile thecal stages, due to a history of independent research. While paleontological names are used throughout this text, known biological affinities for the species counted are given in Table 2. Specimens were classified to the genus level, where species-level identification was not possible. The *Brigantedinium* spp. group is comprised of *Brigantedinium cariacoense* and *Brigantedinium simplex* (their distinctive archeopyles could not always be observed as a result of cyst orientation), as well as other smooth round brown cysts. *Operculodinium centrocarpum sensu* Wall and Dale (1966) counts include rare specimens that are taken to have broken processes rather than to be of *Operculodinium centrocarpum* var. *truncatum* (short process variety). *Protoperidinium nudum* cysts were grouped with *Selenopemphix quanta* as their strong morphological similarity makes them difficult to distinguish. *Spiniferites* spp. incorporates all species of this genus, except *Spiniferites elongatus*, *Spiniferites bentorii* and *Spiniferites mirabilis*. Cyst type-A conforms to the descriptions given in Radi et al. (2007) and Pospelova et al. (2008).

3.3. Statistical analysis

Statistical analysis of dinoflagellate cyst assemblages was performed, using CANOCO 4.5 for Windows (ter Braak and Smilauer, 2002). The scarcity of cysts counted in 3 of the samples (sites 17, 23 and 59) necessitates their exclusion from the analysis, while cysts of all taxa have been included, except rare occurrences of unknown morphotypes. Detrended correspondence analysis (DCA) categorizes variation within the study area as linear, based on a length of the first gradient of 1.161 standard deviation units. Relative proportions of dinoflagellate cyst species and their spatial distribution may therefore be analyzed indirectly with Principal component analysis (PCA) or directly with redundancy analysis (RDA). PCA is a commonly used method for detecting structure in the relationships between species and sample distribution in palynological studies with the extraction of orthogonal principal components from the original variable space, creating a 2D graphical projection. RDA further extends assemblage groupings to detecting the correlation between species distribution and coincident environmental or geochemical parameters, and is performed on the current data set without transformations (Fig. 6). Due to the very high resolution of this study, temperature and salinity are not considered in the RDA since their values have been extrapolated within the World Ocean Atlas, and thus downplay the importance of measured geochemical data. Forward selection was used in order to rank the importance of OC, N, OC/TN and biogenic opal in explaining distribution of dinoflagellate cyst assemblages. Geochemistry is deemed significantly related to species composition for *P*-values less than 0.05. Statistical analysis is not performed on dinoflagellate cyst concentrations, due to the variance in sedimentation rate that must result at different study sites due to the diverse impact of complex local hydrography.

4. Results

4.1. Dinoflagellate cyst abundances and assemblages

Excellent dinoflagellate cyst assemblages have been recovered (with the exception of low cyst counts at sites 17, 23 and 59) and 36 cyst taxa were identified. Total cyst concentrations, calculated as cysts per gram of dry sediment (cysts g^{-1}), range greatly from 100 cysts g^{-1} near the end of the Saanich Peninsula outfall pipe to over 25,000 cysts g^{-1} within the stagnant waters of Victoria Harbour, with an average of 3173 cysts g^{-1} (Fig. 3A). Highest concentrations occur in Victoria Harbour (25,640 cysts g^{-1}), Esquimalt Harbour (15,609–20,063 cysts g^{-1}), followed by an atypical site 35 outside Cadboro Bay (7509 cysts g^{-1}) and at the Saanich Peninsula outfall (5073 cysts g^{-1}).

In general, dinoflagellate cyst assemblages are characterized by a relatively high proportion (average 56%) of cysts produced by heterotrophic dinoflagellates. The most common cysts recorded from heterotrophic taxa include *Brigantedinium*, *Echinidinium* and *Dubridinium* species, *Quinquecuspis concreta*, and cysts of *Polykrikos kofoidii and P. schwartzii* (Fig. 4). Relative proportions of cysts produced by phototrophic species are compared to those from heterotrophic taxa in Fig. 3B, where a distinction is made between the proportion of cysts from species of Protoperidiniaceae and those from *Polykrikos kofoidii/schwartzii* and *Dubridinium* species, due to their acquaintance in recent literature with different environmental signals. The highest proportions of cysts from heterotrophic dinoflagellates are found in Esquimalt (77–79%) and Victoria (70%) Harbours, adjacent to Macaulay Point outfall (site 10, 75%; site 14, 72%, site 17, 71%; site 18, 69%), near Clover Point outfall (site 24, 70%; site 20, 69%; site 22, 64%), and at the

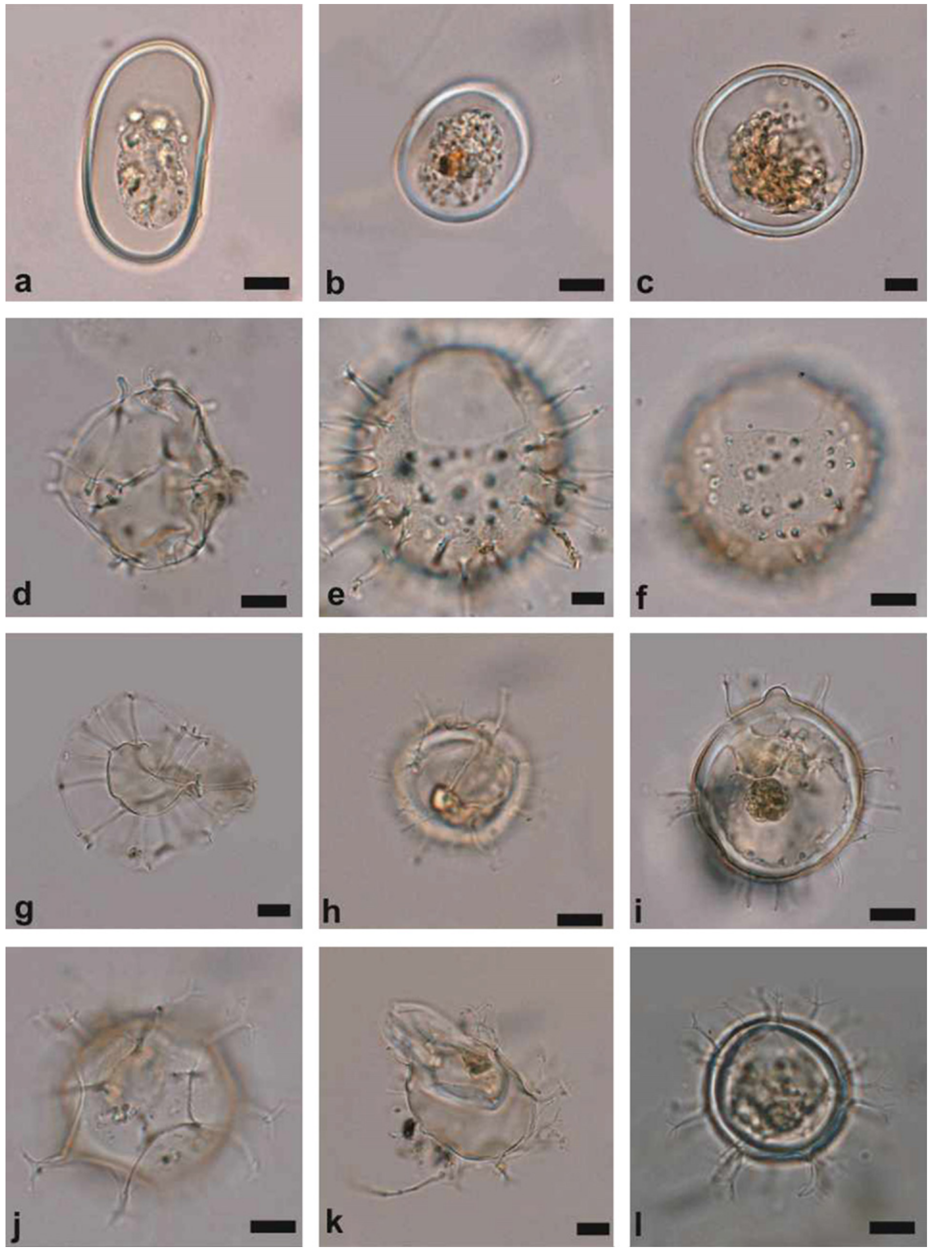

Plate 1. Dinoflagellate cysts from Southern Vancouver Island. Photomicrographs are bright field images. Scalebar = 10 μm. (a) Cyst of *Alexandrium* spp., Clover Point outfall, UVIC 08-022 (P42/1), optical section. (b) cyst of *Alexandrium* spp., off Telegraph Cove–Oak Bay to Cordova Bay region, UVIC 08-037 (K49/0), optical section. (c) Cyst of *Alexandrium* spp. Type B, south of Esquimalt Harbour, UVIC 08-008 (P52/0), optical section. (d) *Impagidinium* spp., Clover Point outfall, UVIC 08-022 (S42/0). (e) *Operculodinium centrocarpum sensu* Wall and Dale (1966), mouth of Esquimalt Harbour, UVIC 08-007 (M35/4), dorsal surface. (f) *Operculodinium centrocarpum* (with broken processes), off Finnerty Cove–Oak Bay to Cordova Bay region, UVIC 08-039 (C33/4), dorsal surface. (g) *Nematosphaeropsis* spp., Clover Point outfall, UVIC 08-026 (T23/0), mid focus. (h) Cyst of *Pentapharsodinium dalei*, Macaulay Point Outfall, UVIC 08-018 (E31/1), mid focus. (i) *Spiniferites bentorii*, Macaulay Point outfall near mouth of Victoria Harbour, UVIC 08-019 (O35/1). (j) *Spiniferites* spp., Clover Point outfall, UVIC 08-024 (M46/2). (k). *Spiniferites* spp. excystment, Macaulay Point Outfall, UVIC 08-018 (W29/3). (l) *Spiniferites* spp., Sidney Channel, UVIC 08-254 (Q35/0).

mouth of Cadboro Bay (69%) (Fig. 3B, Fig. 7). In relation to nearby sites, a relative increase in cysts of *Polykrikos kofoidii/schwartzii* and *Dubridinium* species is also found in the same regions (Fig. 3B, 8C,D). Cysts of the newly described *Protoperidinium tricingulatum* are found almost exclusively within Victoria and Esquimalt Harbours.

In comparison to the dominance of cysts from heterotrophic species at the southern sites, the northerly sites contain much higher proportions of cysts from phototrophic taxa. The most common phototrophic cyst-producing taxa in the study area are *Operculodinium centrocarpum* sensu Wall and Dale (1966), *Pentapharsodinium dalei, Gonyaulax spinifera* complex and *Alexandrium* type species (Fig. 4). The highest proportions of phototrophic species are found within Cadboro Bay (site 33, 72%), at the most northerly sites (54–59, 57–69%), in Saanichton Bay (60%) and southeastward of Macaulay Point outfall (site 11, 52%) (Fig. 3B). The cosmopolitan species *O. centrocarpum* generally increases in abundance in the regions depicted by the most barren representation of cysts of *Polykrikos kofoidii/schwartzii* and *Dubridinium* species (Fig. 4). As a broad trend, the potentially toxic *Alexandrium* species are observed to follow the same pattern, except for striking enhanced cyst production east of Macaulay Point (site 11, 25%), at

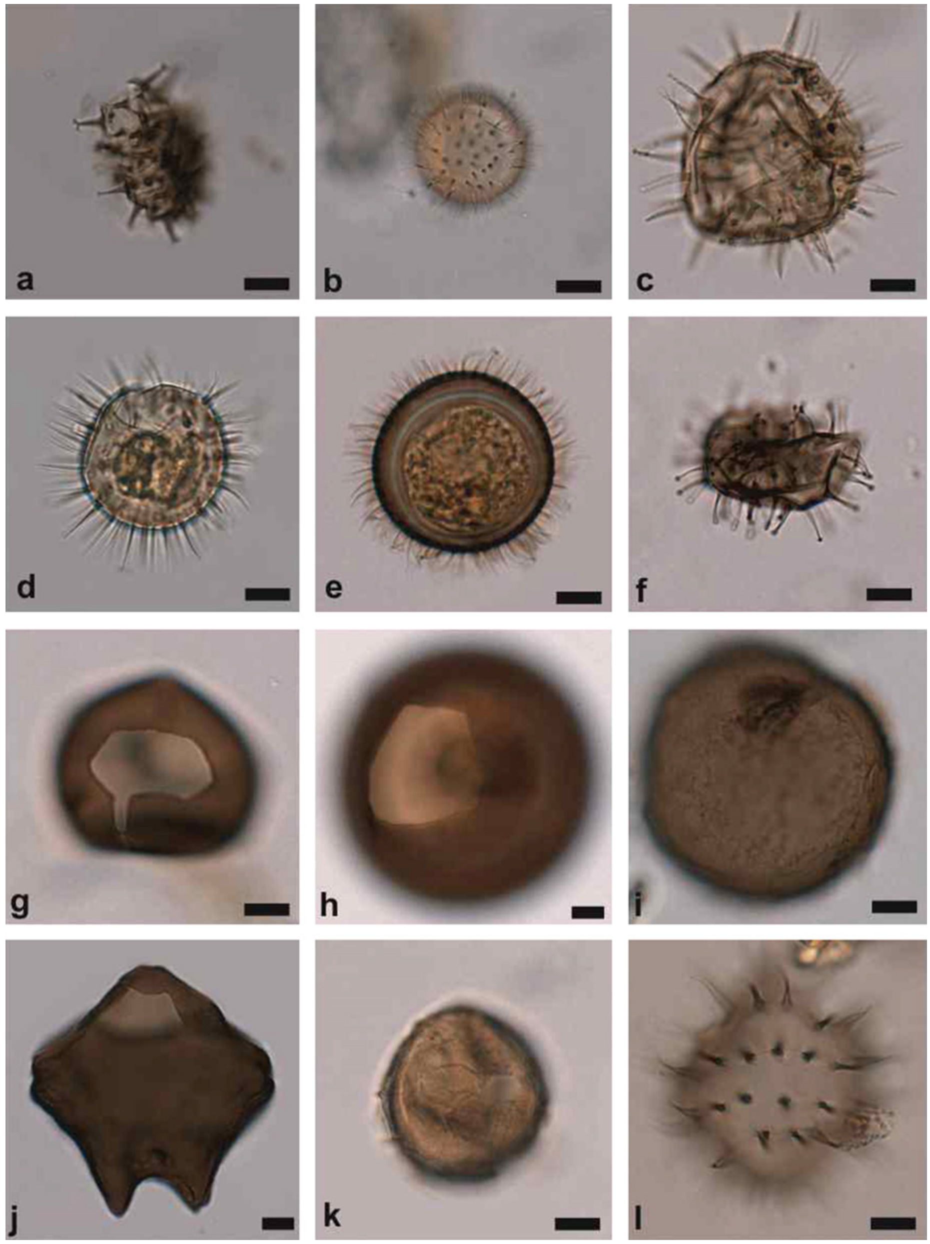

Plate 2. Dinoflagellate cysts from Southern Vancouver Island. Photomicrographs are bright field images. Scalebar = 10 μm. (a) *Echinidinium aculeatum*, Clover Point outfall, UVIC 08-022 (R36/1). (b) *Echinidinium delicatum*, off Finnerty Cove–Oak Bay to Cordova Bay region, UVIC 08-039 (R28/1). (c) *Echinidinium granulatum*, Clover Point outfall, 08-024 (M45/0). (d) *Echinidinium zonneveldiae*, Haro Strait, 08-255 (X47/3). (e) *Echinidinium* spp., Esquimalt Harbour, UVIC 08-006 (K50/3). (f) *Islandinium* ?*minutum* var. *cesare*, Cadboro Bay, UVIC 08-034 (E34/4). (g) *Brigantedinium cariacoence*, Clover Point outfall, UVIC 08-026 (O53/3), dorsal surface. (h) *Brigantedinium simplex*, south of Esquimalt Harbour, UVIC 08-008 (E46/2). (i) *Dubridinium* spp., Esquimalt Harbour, UVIC 08-005 (U36/0). (j) *Quinquecuspis concreta*, Clover Point outfall, UVIC 08-022 (K32/0), dorsal surface. (k) Cyst of *Protoperidinium americanum*, Clover Point outfall, UVIC 08-026 (L37/3), dorsal surface. (l) *Protoperidinium nudum*, Esquimalt Harbour, UVIC 08-006 (C20/2).

the end of Clover Point (site 28, 31%), inside Cadboro Bay (site 33, 25%), and near Saanich Peninsula outfall (site 52, 42%) (Fig. 8A). Occurrences of the other main phototrophic contributors, including *Spiniferites* spp., remain quite varied throughout the region (Fig. 4).

4.2. Geochemical analysis

Distribution of the measured geochemical properties is shown in Fig. 5. Organic carbon values, measured in weight percent of dry sediment ($wt\%_{OC}$), range 0.1–3.8, and average 1.0 $wt\%_{OC}$ (Fig. 5A). Lowest values occur off the Saanich Peninsula outfall (site 52, 0.1 $wt\%_{OC}$), and outside Cadboro Bay (site 35, 0.1 $wt\%_{OC}$), while the greatest percentages of organic carbon are found within Esquimalt Harbour (3.6–3.8 $wt\%_{OC}$), eastward of Macaulay Point (site 10, 2.5 $wt\%_{OC}$; site 11, 2.1 $wt\%_{OC}$) and at the end of Saanich Peninsula outfall (site 49, 1.7 $wt\%_{OC}$) and in Telegraph Cove (site 37, 1.9 $wt\%_{OC}$). The weight percent of biogenic silica in dry sediment ($wt\%_{OPAL}$), used to approximate diatom production, is highest in low-flushing bays and near an effluent release (Fig. 5B). In particular, the greatest values are found in Esquimalt Harbour (9.1–9.6 $wt\%_{OPAL}$), eastward of Macaulay Point outfall (site 18, 7.1 $wt\%_{OPAL}$; site 16, 8.5 $wt\%_{OPAL}$), at the end of Clover Point outfall (site 26, 6.6 $wt\%_{OPAL}$), at the mouth of Cadboro Bay (8.0 $wt\%_{OPAL}$), in Telegraph cove (site 37, 9.4 $wt\%_{OPAL}$), and at Saanich Peninsula outfall (site 49, 8.9 $wt\%_{OPAL}$). Local values range from 3.2 (site 55 in Haro Strait) to 9.6 (Esquimalt Harbour), with an average of 6.2 $wt\%_{OPAL}$ throughout the study area. Organic carbon to nitrogen ratios (OC/TN) range from an anomalously low value

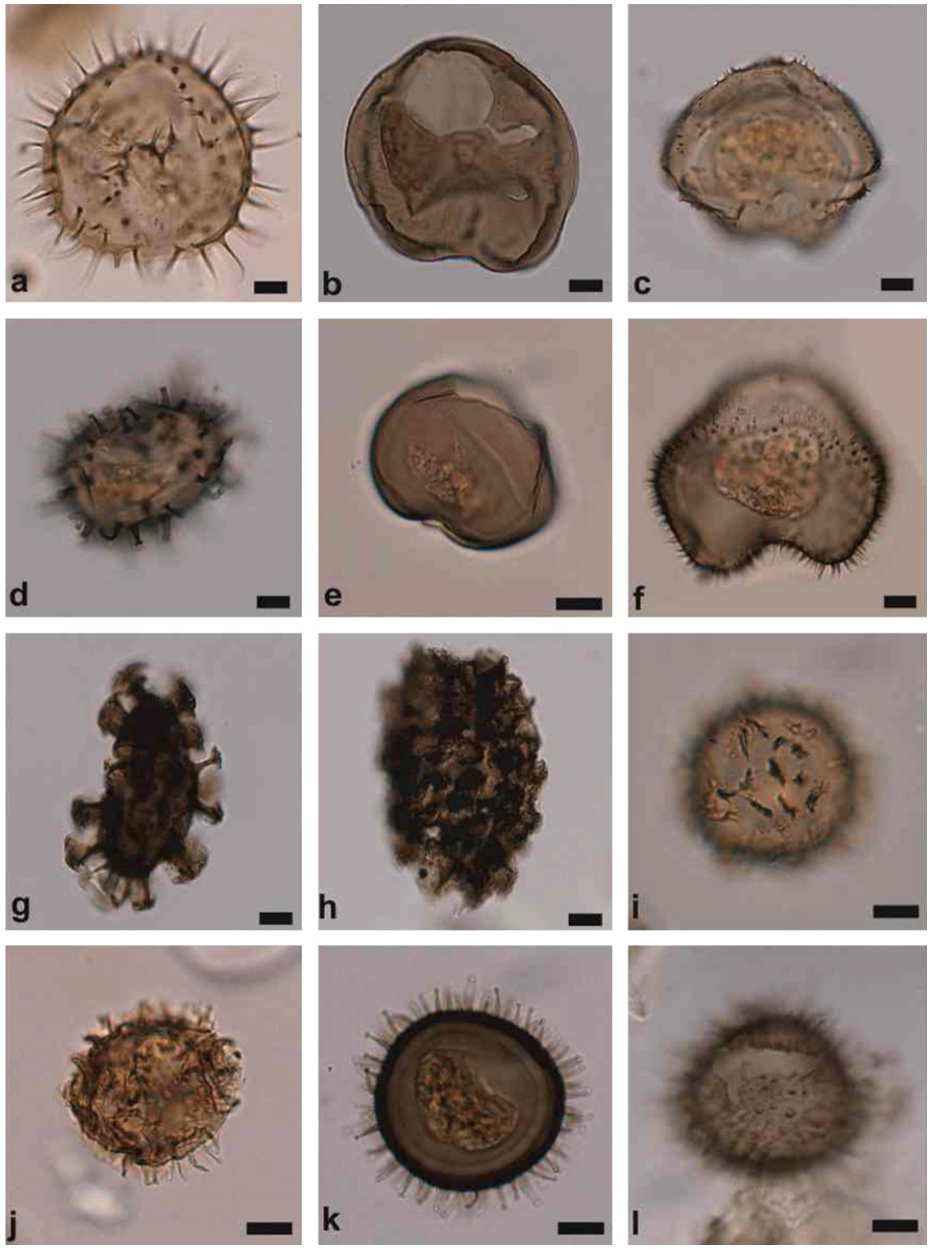

Plate 3. Dinoflagellate cysts from Southern Vancouver Island. Photomicrographs are bright field images. Scalebar = 10 μm. (a) *Selenopemphix quanta*, Macaulay Point outfall, UVIC 08-018 (E35/1), dorsal surface. (b) *Selenopemphix nephroides*, Macaulay Point outfall near mouth of Victoria Harbour, UVIC 08-019 (M21/1), dorsal surface. (c) *Trinovantedinium applanatum*, off Finnerty Cove–Oak Bay to Cordova Bay region, UVIC 08-039 (R27/4), ventral surface. (d) *Trinovantedinium variable*, south of Esquimalt Harbour, UVIC 08-008 (S21/3). (e) *Votadinium calvum*, Esquimalt Harbour, UVIC 08-006 (D51/0). (f) *Votadinium spinosum*, Esquimalt Harbour, UVIC 08-006 (A46/2). (g) Cyst of *Polykrikos schwartzii* sensu Matsuoka et al. (2009), off Finnerty Cove–Oak Bay to Cordova Bay region, UVIC 08-039 (N40/0), lateral surface. (h) Cyst of *Polykrikos kofoidii* sensu Matsuoka et al. (2009), Esquimalt Harbour, UVIC 08-006 (J39/4), lateral surface. (i) Cyst Type-A, Macaulay Point outfall, UVIC 08-018 (V29/3). (j) Cyst Type-A, Clover Point outfall, UVIC 08-026 (J34/1). (k) Cyst Type C, Esquimalt Harbour, UVIC 08-006 (M19/0). (l) Cyst Type C, Esquimalt Harbour, UVIC 08-005 (U40/2).

outside Cadboro Bay (site 35, OC/TN ~ 0.4) to maximums found immediately eastward of Macaulay Point outfall (site 11, OC/TN ~ 18; site 11, OC/TN ~ 22) (Fig. 5D). Other high values occur inside Esquimalt Harbour (OC/TN ~ 13–15), and at the terminus of Clover Point outfall (site 26, OC/TN ~ 10), while ratios at all other sites vary within a range 6.3–9.8.

4.3. Statistical analysis

The results of the Redundancy Analysis (RDA) demonstrate that the first ordination axis, which explains 55.4% of the variance, is positively and significantly correlated with biogenic opal given a *P*-value of 0.002 (Fig. 6). A Monte Carlo permutation test under the reduced model with 499 permutations demonstrates that the first ordination axis is significant with *P*-value of 0.050. The arrangement of cyst species along the first axis shows a positive ordination for the majority of heterotrophs and a negative ordination of almost all phototrophs, with *Alexandrium* species demonstrating the strongest negative ordination and a strong negative correlation to biogenic opal. The few heterotrophic species denoting negative ordination show relatively low correlation and are low in abundance overall. Distribution of sample sites demonstrates that sites associated with higher relative abundance of cysts from heterotrophic dinoflagellates, inclusive of those from Esquimalt Harbour, east of Macaulay Point outfall and at the

Table 2
Taxonomic designation of dinoflagellate cysts recorded in this study.

Family	Cyst species (paleontological name)	Dinoflagellate thecal name or affinity (biological name)
	Phototrophic	
Gonyaulacaceae	–	*Alexandrium tamarense* and spp.
	Impagidinium spp.	*Gonyaulax* sp. indet.
	Nematosphaeropsis labyrinthus	*Gonyaulax spinifera* complex
	Operculodinium centrocarpum sensu Wall & Dale 1966	*Protoceratium reticulatum*
	Spiniferites elongatus	*Gonyaulax spinifera* complex
	Spiniferites bentorii	*Gonyaulax spinifera* complex
	Spiniferites mirabilis	*Gonyaulax spinifera* complex
	Spiniferites spp.	*Gonyaulax* spp. indet.
Perdiniaceae	–	*Pentapharsodinium daleii*
	Heterotrophic	
Diplopsalidaceae	*Dubridinium* spp.	Diplopsalid group
Polykrikaceae	Cyst of *Polykrikos kofoidii* sensu Matsuoka et al., 2009	*Polykrikos kofoidii*
	Cyst of *Polykrikos schwartzii* sensu Matsuoka et al., 2009	*Polykrikos schwartzii*
Protoperidiniaceae	*Brigantedinium cariacoense*	*Protoperidinium avellanum*
	Brigantedinium simplex	*?Protoperidinium conicoides*
	Total *Brigantedinium*	*Protoperidinium* spp.
	Echinidinium aculeatum	*Protoperidinium* sp. indet.
	Echinidinium delicatum	*Protoperidinium* sp. indet.
	Echinidinium granulatum	*Protoperidinium* sp. indet.
	Echinidinum zonneveldiae	*Protoperidinium* sp. indet.
	Echinidinum spp.	*Protoperidinium* sp. indet.
	Islandinium brevispinosum	*Protoperidinium* sp. indet.
	Islandinium ?minutum var. cesare	*Protoperidinium* sp. indet.
	–	*Protoperidinium americanum*
	–	*Protoperidinium nudum*
	Cyst of *Protoperidinium tricingulatum*	*Protoperidinium tricingulatum*
	Protoperidinium spp.	*Protoperidinium* spp. indet.
	Quinquecuspis concreta	*Protoperidinium leonis*
	Selenopemphix nephroids	*?Protoperidinium sp. (Conica group)*
	Selenopemphix quanta	*Protoperidinium conicum; P. nudum*
	Trinovantedinium applanatum	*Protoperidinium pentagonum*
	Trinovantedinium variabile	*Protoperidinium* sp. indet.
	Votadinium calvum	*Protoperidinium oblongum*
	Votadinium spinosum	*Protoperidinium claudicans*
Indeterminant	Cyst Type-A	*?Protoperidinium* sp. indet.
	Spiny brown	*?Protoperidinium* sp. indet.

Thecal equivalents are taken from Head (1996), Zonneveld (1997), Head (2002), Head et al. (2001), Pospelova and Head (2002), Kawami et al. (2009) and Matsuoka et al. (2009).

mouth of Cadboro Bay are associated with the strongest positive ordination on the first axis, while the most negatively ordinated sites contain the greatest percentage of phototrophic dinocysts. Rankings for the value of each individual geochemical variable (marginal effect) and the importance of cumulative geochemical groupings (conditional effect) on the basis of fit are included in Fig. 6. Although OC, N and OC/TN are found to be statistically insignificant by *P*-values of 0.182, 0.304 and 0.204 respectively, they align positively with the first ordination axis, along with biogenic opal values, and cluster with the cysts produced by *Polykrikos, Echinidinium, Dubridinium* and *Brigantedinium* dinoflagellate species. The second ordination axis, which explains an additional 29.3% of the variance, is not significantly correlated to any of the geochemical variables, and shows no distinct clustering between related sites.

5. Discussion

Dinoflagellate cyst abundance, the proportion of cysts produced by heterotrophic and phototrophic dinoflagellates and the composition of cyst assemblages are known to reflect spatial variation in abiotic factors (e.g. Dale, 1996, 2009; Harland et al., 1998; Dale et al., 1999; Rochon et al. 1999; Matsuoka, 1999; de Vernal et al., 2001, 2005; Pospelova et al., 2004, 2008; Radi and de Vernal, 2004; Harland et al., 2006; Radi et al., 2007; Bouimetarhan et al., 2009; Zonneveld et al., 2009; Holzwarth et al., 2010; Pospelova and Kim, 2010). These environmental signals can only be interpreted once it has been established that the assemblages have not been systematically biased by the selective preservation of more resistant cysts (Dale, 1976; Zonneveld et al., 1997; Versteegh and Zonneveld, 2002; Zonneveld et al., 2007, 2008). We deem that discriminatory preservation is unlikely to have affected the signals reported here, as the records from this study are not noticeably affected by selective oxidative degeneration. No dinocyst samples from the study area contained a perceptible amount of broken cysts, or exhibited bleaching or disintegration of the *Protoperidinium* (i.e. *Brigantedinium* spp.) or *Echinidinium* species that have been designated as sensitive to oxygen degradation (Dale, 1976; Zonneveld et al., 1997; Versteegh and Zonneveld, 2002; Zonneveld et al., 2007, 2008). They rather contain exquisitely preserved cysts from all taxa. Further, high sedimentation rates in the area allow for fast burial, thus restricting contact time between dinoflagellate cysts and oxygenated bottom waters (Lavelle et al., 1986; Johannessen et al., 2003).

It must also be noted that dinoflagellate cyst abundances in sediment do not provide unequivocal records of dinoflagellate production, which would require quantification of both species-level cyst production and localized sediment accumulation rates. Regionally, sediment trap data or ^{210}Pb derived sedimentation rates are only available for the nearby Strait of Georgia

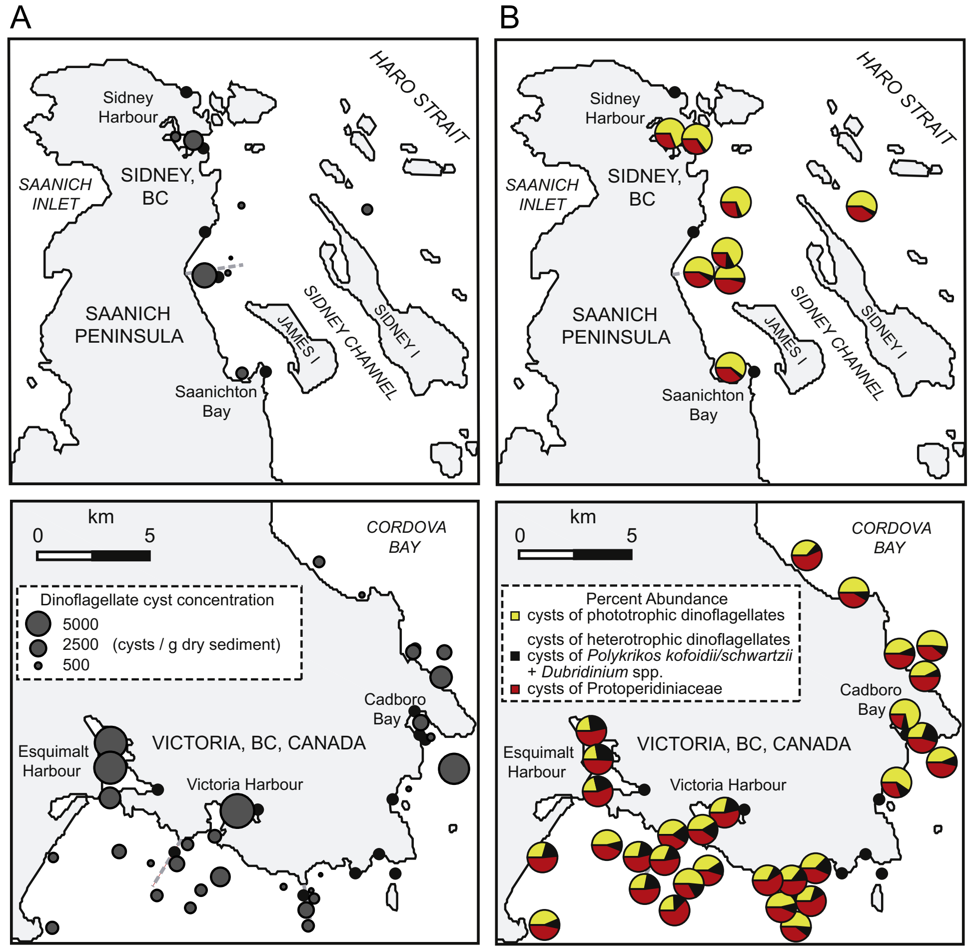

Fig. 3. Dinoflagellate cyst distribution of (A) total concentrations (cysts g^{-1}) and (B) relative abundance (%) of cysts produced by phototrophic and heterotrophic (cysts of *Polykrikos kofoidii/schwartzii* and *Dubridinium* spp. versus Protoperidiniaceae) dinoflagellates, in relation to sewage outfall (dashed lines) and stormwater discharge stations (black dots).

(0.94–2.94 cm yr^{-1}, Johannessen et al., 2003) and Puget Sound (0.5–2.48 cm yr^{-1}, Lavelle et al., 1986). While the most robust productivity proxy is based on a flux (per unit time) of dinoflagellate cysts, concentration measurements in cysts per gram dry do allow for estimates of relative increases or decreases in cyst production, where sedimentation rates are constant. Here, an absolute abundance of dinoflagellate cysts is taken to be comparable for neighboring sites denoted by similar grain size, since cyst diversity remains comparable. For example, whereas the higher energy sites near Clover Point and Saanich Peninsula outfalls, denoted by larger grain sizes (Table 1) and greater tidal exchange (Fig. 1), likely under-represent productivity compared to lower energy sites, due to greater transport of minute particles, outfall impact in these locations can nevertheless be seen in relation to adjacent sites.

Sedimentary geochemistry supplies additional clues about environmental conditions. Biogenic opal concentrations are a proxy for biosiliceous productivity, as they are known to correlate well provided that $Si(OH)_4$ is never limiting in the surface waters and that sedimentation rate is high enough to quickly bury any particulate organic matter that is rained down (Nelson et al., 1995; Ragueneau et al., 2000). This biosiliceous production is dominantly attributed to diatoms in highly productive coastal upwelling zones, with minor contributions derived from silicoflagellates and radiolarians (Nelson et al., 1995; Ragueneau et al., 2000). Here, we find a statistically significant correlation between biogenic opal and cysts from heterotrophic dinoflagellates (Fig. 6). While these proxies are also associated with organic carbon (often linked to relative production in the water column) and nitrogen concentration (commonly used to denote nutrient abundance) (e.g. Pedersen and Calvert, 1990; McQuoid et al., 2001), the relationships are found to be statistically insignificant. Biogenic opal is likely grouped with specific species, due to the disparate feeding habits of different dinoflagellates.

In coastal regions with available dissolved silica, diatoms are typically the first phytoplankton group to prosper from available nutrients, while phototrophic dinoflagellates become more competitive once the availability of dissolved silica wanes (Matsuoka, 1999). These species may also prosper with an increased light availability, due to diminished diatom production or turbidity. In the present study, a general decrease in biogenic opal concentration is seen in sites with greater proportions of cysts from phototrophic dinoflagellates (Fig. 6). Heterotrophic dinoflagellates are selective feeders that consume prey cells that may be many times their size (Jacobson and Anderson, 1986). It has been suggested that while Polykrikaceae and Diplopsalid species consume a more mixed diet, Protoperidinoids display a preference for both solitary and colonial diatoms (Jacobson and Anderson, 1986; Jeong et al., 2001; Matsuoka et al., 2003). As expected, an increased concentration of *Protoperidinium* cysts is typically consistent with the prosperity of diatoms in high-nutrient, upwelling regions (Wall et al., 1977; Dale, 1996; Harland et al., 1998; Zonneveld et al., 2001; Dale et al., 2002; Reichart and Brinkhuis, 2003; Marret and Zonneveld, 2003; Pospelova et al., 2006, 2008; Holzwarth et al., 2007; Marret et al., 2008; Bouimetarhan et al., 2009; Holzwarth et al., 2010).

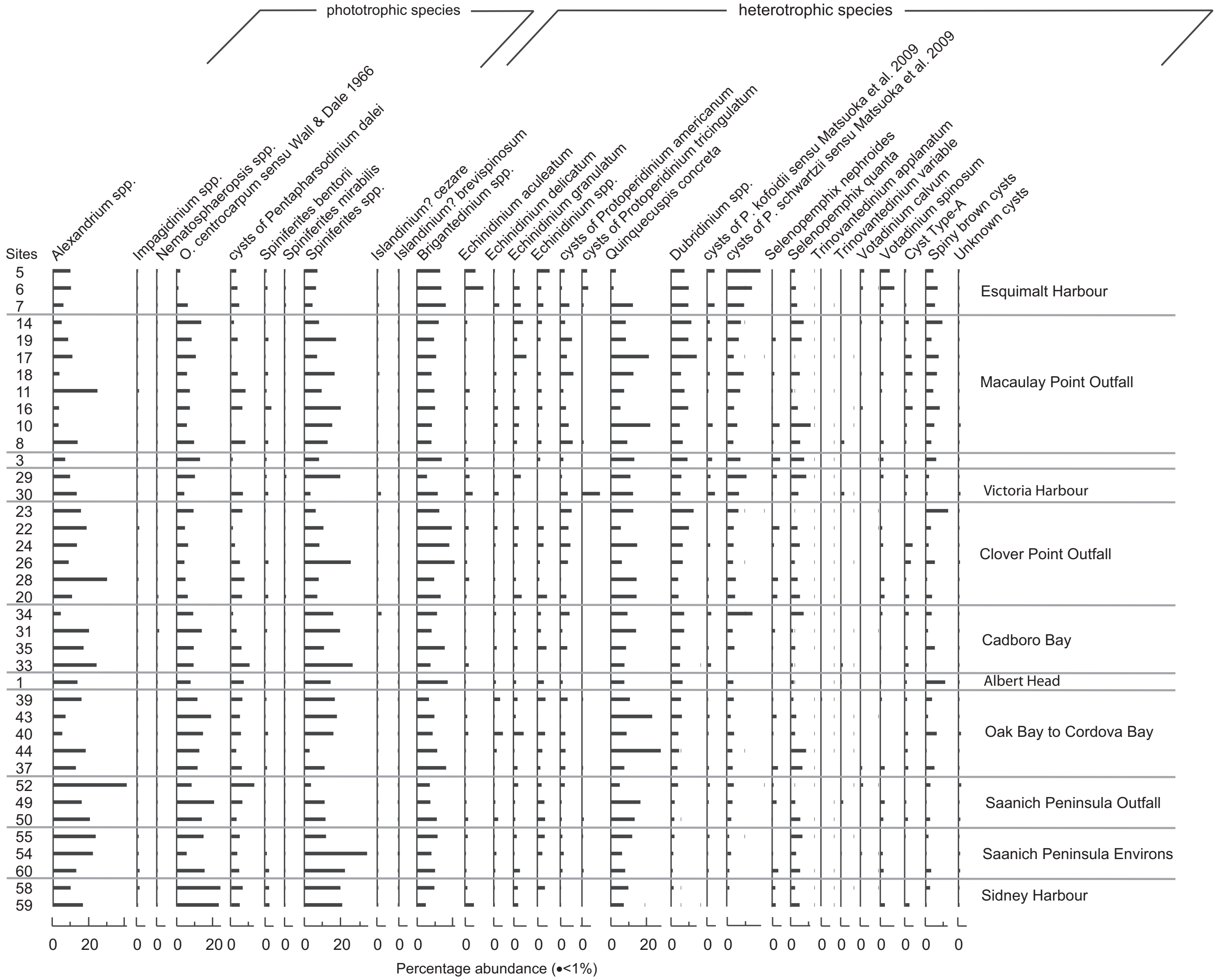

Fig. 4. Percent abundance diagram of dinoflagellate cyst taxa counted. Regions are sorted based on relative abundance of cysts of *Polykrikos kofoidii/schwartzii* plus *Dubridinium* species, from highest (top) to lowest (bottom).

It is important to compare the patterns of dinoflagellate cyst distribution observed in this work with previous studies. Dinocyst records from several coastal areas and estuaries that are known to be affected by anthropogenic nutrient input contain high proportions of cysts from heterotrophic dinoflagellates, often characterized by a marked increase in cysts of *Polykrikos kofoidii and schwartzii* and *Dubridinium* species (Matsuoka, 1999; Pospelova et al., 2002, 2005; Matsuoka et al., 2003; Ellegaard et al., 2006; Dale, 2009). Such studies include time-series analyses of recent sediment core samples (Matsuoka, 1999; Pospelova et al., 2002; Ellegaard et al., 2006) and examinations of spatial distribution in surface sediment samples (Matsuoka et al., 2003; Pospelova et al., 2005). Sample material for these studies originates from Japan, eastern Unites States and Denmark, suggesting that the signal is not area-specific. To date, the analysis of surface sediment samples from three embayments in relation to sewage outfall locations, on the east coast of the United States, provides the only comparable study (Pospelova et al., 2005). While the present study likewise points to a qualitative association between the proportion of cysts produced by heterotrophic dinoflagellates (specifically of *Polykrikos kofoidii/schwartzii* and *Dubridinium* species) and nutrient gradients in the system, the complex hydrological configuration renders it impossible to quantify this link by correlating the proportion of these species with distance to the point sources of nutrient enrichment. Nevertheless, Fig. 7(C and D) shows that *Polykrikos kofoidii/schwartzii* and *Dubridinium* species generally increase in the proximity to the points of nutrient enrichment.

Despite dispersal by a dynamic hydrological system, effects of nutrient loading by sewage and/or stormwater effluent are identified in the cyst-based eutrophication signal discussed above (albeit at the qualitative level). A nested 3D water quality model used to assess the neutral buoyancy trapping depth and dilution factors of sewage effluent plumes from Macaulay and Clover Point outfalls estimates horizontal impact zones to be contained within 100 of discharge with a plume width of up to 237 m (Hodgins et al., 1998; Hodgins, 2006). Trends found in monitored benthic biota and sediment chemistry, however, evidence primary outfall effects <800 m eastward of Macaulay Point and about 200 m eastward of Clover Point, with lesser impacts recorded in shallower shoreward regions (CRD, 2000; Stubblefield et al., 2006; CRD, 2008b). Results from this study also clearly indicate a much larger impact zone than predicted by modeling.

Long-term current measurements collected mid-depth at each outfall station help elucidate adjacent areas likely to be most

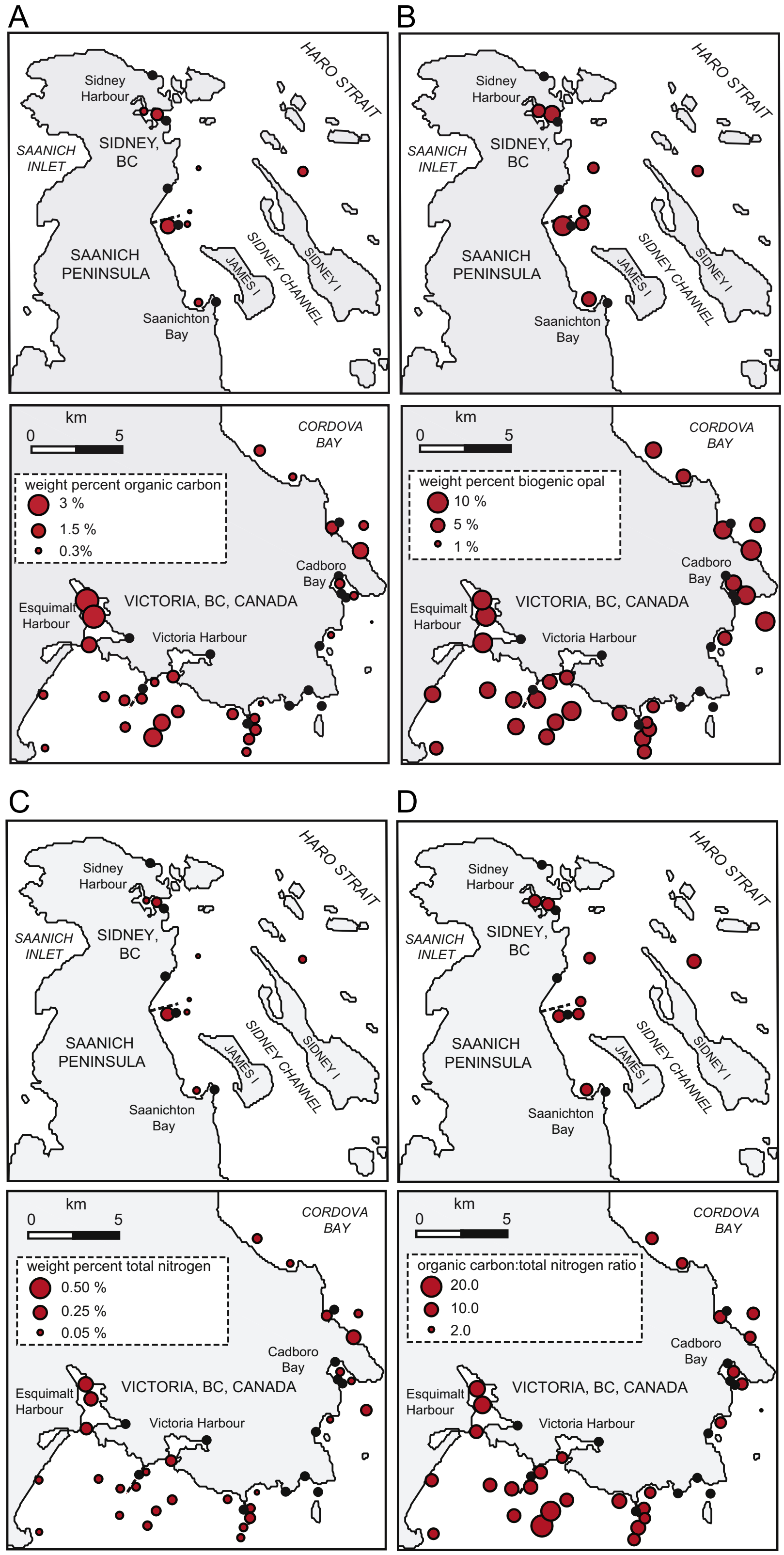

Fig. 5. Sedimentary geochemical property distribution of (A) organic carbon (wt%), (B) biogenic opal (wt%), (C) total nitrogen (wt%) and (D) the ratio of organic carbon to total nitrogen, in relation to sewage outfall (dashed lines) and stormwater discharge stations (black dots).

impacted by an effluent release. The zone eastward of Clover Point is thus predicted to be at the greatest risk of an effluent impact due to *E* flowing currents of up to 115 cm s^{-1} occurring most frequently, with 54% of all current flow observations (Chandler, 1997). Clover Point findings include some of the highest proportions of cysts from heterotrophic dinoflagellates (Fig. 3B) with relatively higher proportions of cysts from both *Dubridinium and Polykrikos* species (Fig. 7C and D). However, the impact area is found shoreward of discharge, near the planned stormwater discharge site, rather than near sewage outfall. High concentrations

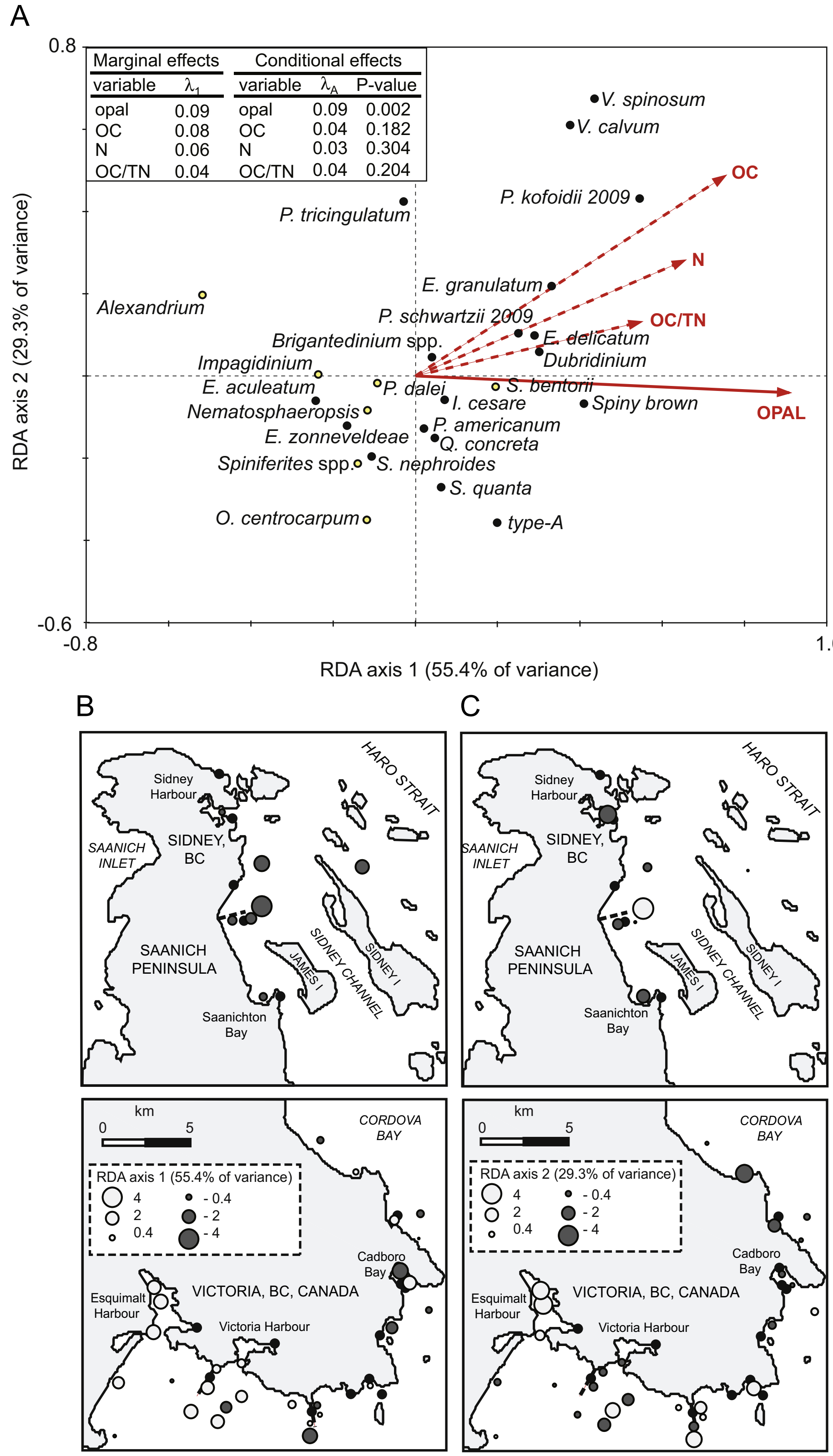

Fig. 6. Principle component analysis generated diagram (A) showing the ordination of taxa on axes 1 (horizontal) and 2 (vertical), which explains 32.2% and 24.3% of the variance, respectively. Cysts of heterotrophic taxa are shown with black circles, while cysts of phototrophic species are shown in light circles. (B) PCA axis 1 and (C) PCA axis 2 spatial distribution of sample site ordination values, in relation to sewage outfall (dashed lines) and stormwater discharge stations (black dots).

of biogenic opal (Fig. 5B) and OC/TN ratio (Fig. 5D) are located at the point of an effluent release.

The zone southeast of Macaulay Point is expected to denote the greatest degree of influence from a outfall discharge, since SE flowing currents of up to 1.5 knots (78 cm s^{-1}) occur most frequently with 31% of all current data (Chandler, 1997). Our results from the Macaulay Point region again include some of the highest proportions of cysts from heterotrophic dinoflagellates

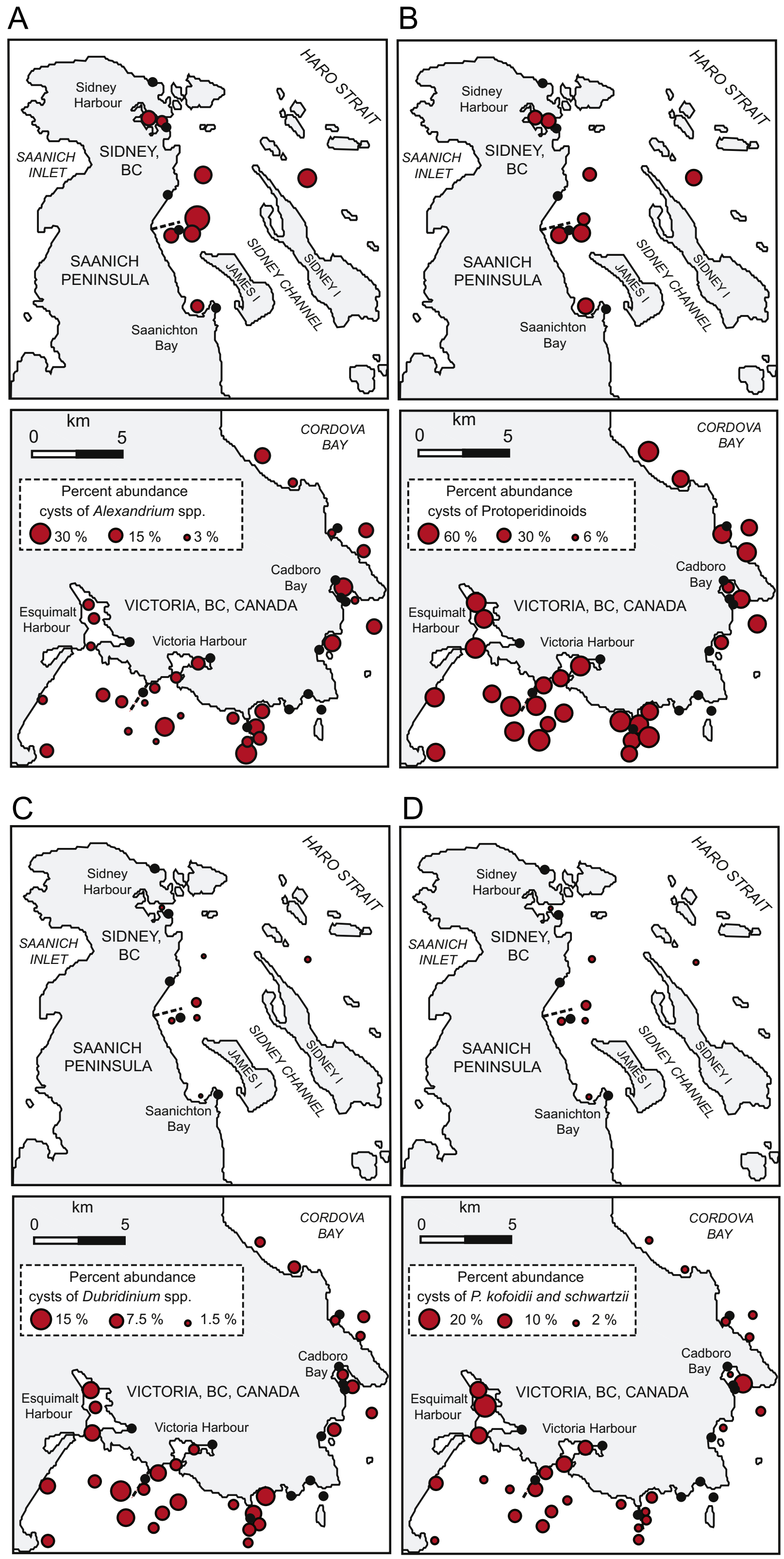

Fig. 7. Spatial distribution of percent abundance of cysts produced by (A) *Alexandrium* species, (B) Protoperidiniaceae, (C) *Dubridinium* species, and (D) *Polykrikos kofoidii* and *Polykrikos schwartzii*, in relation to sewage outfall (dashed lines) and stormwater discharge stations (black dots).

(Fig. 3B) with the highest proportion of cysts from of *Dubridinium* spp. in the study area (14%), and strong representation of both *Dubridinium and Polykrikos* species in relation to the environs (Fig. 7C and D). Geochemistry data further corroborates a cyst-based eutrophication signal with some of the highest concentrations of organic carbon (Fig. 5A) and biogenic opal (Fig. 5B), along with OC/TN ratio maximums (Fig. 5D). The impact area appears to be contained within approximately 2 km SE and directly NW of Macaulay outfall, although differentiation between effects from sewage outfall and overflow is not possible in this region. Macaulay Point sewage input appears to affect dinoflagellate cyst assemblages and abundance to a greater degree, despite a greater volumetric discharge of sewage from Clover Point (Fig. 3). This likely results from an effluent being flushed less rapidly from the amphidromic region that it is subjected only to the diurnal cycle tidal range (Thomson et al., 2007; Foreman et al., 1995). With future population growth on the southern Vancouver Island, outfall from Macaulay Point is predicted to more than double by the year 2045, with a nearly constant effluent discharge maintained at Clover Point for the same time period (Stubblefield et al., 2006). As this site already demonstrates deficient assimilative capacity by recognized dinoflagellate cyst-based signs of eutrophication, a doubling of point source nutrient input would have a significant and concerning impact on the receiving environment.

Monthly monitoring of the Bazan Bay receiving environment has detected no appreciable effects from the Saanich Peninsula secondary sewage treatment plant effluent compared to their Haro Strait reference station (located nearby this study's site 55, see Fig. 2) (CRD, 2008a). Plume modeling predicts the impact zone to be constrained to within 100 m north of discharge (CRD, 2008a), which coincides with current meter data at the outfall. Primarily, tidal currents in excess of 2 knots (100 cm s^{-1}) flowing NNE and N account for 48% of all current flow observations, thus indicating that the effluent plume is most likely to have the greatest effect directly north of outfall discharge (Chandler and Gormican, 2001). Results for this area include some of the greatest percentages of organic carbon (Fig. 5A) and biogenic opal (Fig. 5B) directly at the point of both sewage effluent and planned stormwater release, with somewhat elevated proportions of cysts from both *Dubridinium and Polykrikos* species eastward of discharge (Fig. 7C and D).

Both Victoria and Esquimalt Harbours are marked by a substantial increase in dinocyst abundance per gram dry sediment, the highest proportions of cysts from heterotrophic dinoflagellates (Fig. 3B) and a clear increase in proportions of cysts from both *Dubridinium and Polykrikos* species (Fig. 7C and D). Esquimalt Harbour also contains the greatest percentages of organic carbon (Fig. 5A) and the diatomaceous proxy biogenic opal (Fig. 5B), along with high OC/TN ratios (Fig. 5D). While geochemistry was not analyzed on the Victoria Harbour sample, results are hypothesized to be similar to those of Esquimalt Harbour based on similar hydrology and comparable resultant dinoflagellate cyst abundance and assemblages. These results are not unexpected considering the input of stormwater discharge and proximity to the most highly populated urban centers in the study area.

Several other sites in the study area also exhibit noticeable results. Relatively higher dinoflagellate cyst abundance coupled with increased proportions of cysts from both *Dubridinium and Polykrikos* species (Fig. 7C, D) are also observed at site 3, which may result from its proximity to Esquimalt Harbour, Macaulay Point, or from terrestrial runoff. At the mouth of Cadboro Bay, the sensitivity of the receiving area to wastewater overflow is rated as low based on the benthic biota (CRD, 2000), yet dinoflagellate cyst abundance is significantly lower than the average of the study area (639 versus 3173 cysts g^{-1}) with marked increase in relative proportions in cysts of heterotrophic taxa, particularly in *Dubridinium and Polykrikos* species (Fig. 7C, D). Two planned stormwater outfalls periodically release an effluent directly into the upper surface waters here, which likely impact dinoflagellate production and the subsequent dinocyst assemblage. Noticeably, low concentrations may possibly result from strong tidal flow through the mouth of the bay. In contrast, results from site 35 outside of Cadboro Bay show double the average absolute abundance of cysts per gram dry sediment and an assemblage dominated by Protoperidinoid heterotrophic cysts that are more typical of a region of coastal upwelling (Fig. 3). Here, we propose that constraint of tidal movement, between Ten Mile Point north of Cadboro Bay and the nearby Trial Islands (Fig. 1), results in considerable re-suspension of sediment or the surfacing of bottom water from offshore upwelling that brings additional nutrients to the surface and subsequently drives an enhanced production. This hypothesis is substantiated by an anomalously low organic carbon to total nitrogen ratio of 0.4 (Fig. 5D), which suggests the highest rate of autochthonous production in the study region (Meyers, 1994).

Harmful algal blooms of *Alexandrium* dinoflagellate species that produce saxitoxin, which cause paralytic shellfish poisoning, are increasing in the Pacific Northwest inclusive of Juan de Fuca Strait (Mudie et al., 2002; Anderson et al., 2008). Certain occurrences have been linked to contemporaneous municipal sewage spills or failing septic systems in the nearby Puget Sound (Anderson et al., 2008). Examining the relative abundance of cysts of *Alexandrium* in our samples (Fig. 7A), we find noticeable enhancement of this species at sites 11, 28 and 52 that are adjacent to outfall discharge sites. At first sight, this might seem almost contradictory to the RDA, which indicates an anti-correlation of cysts of *Alexandrium* with nutrient content. However, since such enhancement occurs only in a small set of the overall array of samples, there is no contradiction. This pattern of *Alexandrium* distribution – enhancement of abundance near the point sources of nutrient loading – should be investigated more thoroughly in other coastal locations heavily influenced by human activity, due to the role of this species in harmful algal blooms.

Given the patterns of cyst distribution observed in this study, we cautiously predict that should the discharge of planned secondary sewage treatment plant(s) effluent be released into an area with more restricted water circulation, a significant increase of heterotrophic dinoflagellates (with marked increase in cysts of *Polykrikos kofoidii and schwartzii* and *Dubridinium* species) around the treated sewage water discharge points would result. Nutrient enrichment may also impact a much larger area and lead to the significant changes in the phytoplankton population. To have a more quantitative prediction, the results of this study should be merged with some numerical modeling of the nutrient propagation from the source.

6. Conclusions

Sustainable management of urban coastlines requires detailed knowledge on both natural and anthropogenically driven forcings that enact an environmental change. Here, dinoflagellate cyst assemblages and coincident geochemistry are analyzed at a very high spatial scale (50–100 m between sites), in order to uniquely investigate the near-shore effects of anthropogenic effluent on phytoplankton, within a particularly complex and dynamic hydrographic system. Our study finds that despite dispersal by strong tidal currents and mixing of high-nutrient oceanic input into the prevailing estuarine circulation, the cyst-based eutrophication signal consisting of elevated proportions of *Polykrikos kofoidii* and *schwartzii* and *Dubridinium* species has been recorded near sewage nutrient inputs. The impact of anthropogenic nutrient additions from sewage and stormwater discharge on phytoplankton in the receiving environment, as evidenced by abundances and assemblages of dinoflagellate cysts in coastal sediment samples, is primarily seen in Victoria and Esquimalt Harbours, at the mouth of Cadboro Bay and near effluent outfalls at Macaulay and Clover Points, and Saanich Peninsula. Geochemistry data further substantiates the cyst-based eutrophication signal with high concentrations of organic carbon and biogenic opal, along with OC/TN ratio maximums in similar locations. Enhanced abundance of cysts from toxic (i.e. *Alexandrium*) species in three sites in the near proximity to sewage outfalls represents an interesting pattern that deserves further investigation.

Acknowledgements

We thank Captain Brown and crew of the MSV Strickland for facilitating two very successful cruises, the UBC Inorganic Geochemical Laboratory for biogenic opal and inorganic carbon analysis, Kim Picard of NRCan and the Bedford Institute of Oceanography Sedimentary Laboratory for grain size analysis and Peter Chandler of the Institute of Ocean Sciences for providing current results from the CRD Mooring Program. The Natural Sciences and Engineering Research Council of Canada (NSERC) provided funding for this work.

References

Anderson, D.M., Burkholder, J.M., Cochlan, W.P., Glibert, P.M., Gobler, C.J., Heil, C.A., Kudela, R.M., Parsons, M.L., Rensel, J.E.J., Townsend, D.W., Trainer, V.L., Vargo, G.A., 2008. Harmful algal blooms and eutrophication: examining linkages from selected coastal regions of the United States. Harmful Algae 8, 39–53.

Bouimetarhan, I., Marret, F., Dupont, L., Zonneveld, K.A.F., 2009. Dinoflagellate cyst distribution in marine surface sediments off West Africa (17–6 °N) in relation to sea-surface conditions, freshwater input and seasonal coastal upwelling. Marine Micropaleontology 71, 113–130.

Boyer, T.P., Stephens, C., Antonov, J.L., Conkright, M.E., Locarnini, R.A., O'Brien, T.D., Garcia, H.E., 2002. World Ocean Atlas 2001, Volume 2: Salinity. In: Levitus, S. (Ed.), NOAA Atlas NESDIS 50. U.S. Government Printing Office, Wash., D.C.

Capital Regional District (CRD) Environmental Services Department, 2000. Core area liquid waste management plan. Available at: 〈http://www.crd.bc.ca/wastewater/lwmp/index.htm〉.

Capital Regional District (CRD) Environmental Services Department, 2007. Saanich Peninsula liquid waste management plan, amended and consolidated version. Available at: 〈http://www.crd.bc.ca/wastewater/lwmp/index.htm〉.

Capital Regional District (CRD) Marine Programs, 2008a. Saanich Peninsula treatment plant wastewater and marine environment program, Annual Report 2007. Available at: 〈http://www.crd.bc.ca/wastewater/lwmp/index.htm〉.

Capital Regional District (CRD) Marine Programs, 2008b. Macaulay and Clover Point wastewater and marine environment program, Annual Report 2007. Available at: 〈http://www.crd.bc.ca/wastewater/lwmp/index.htm〉.

Capital Regional District (CRD) Marine Programs, 2008c. CRD Stormwater Quality Annual Report, Saanich Peninsula-2008, Appendix A. Available at: 〈http://www.crd.bc.ca/wastewater/lwmp/index.htm〉.

Chandler, P., 1997. Summary of the CRD mooring program – Victoria, B.C. – 1997–1996. Madeira Research, prepared for Capital Regional District (CRD) Scientific Program.

Chandler, P., Gormican, S.J., 2001. Post-discharge marine assessment program for the Saanich Peninsula treatment plant wastewater outfall. Available at: 〈http://www.crd.bc.ca/wastewater/lwmp/index.htm〉.

Chapman, P.M., 2006. Science, politics and ideology—The Victoria (BC, Canada) sewage issue. Marine Pollution Bulletin 52, 719–721.

Conkright, M.E., Locarnini, R.A., Garcia, H.E., O'Brien, T.D., Boyer, T.P., Stephens, C., Antonov, J.L., 2002. World Ocean Atlas 2001: objective analyses, data statistics, and figures, CD-ROM Documentation. National Oceanographic Data Center, Silver Spring, MD.

Dale, B., 1976. Cyst formation, sedimentation, and preservation: factors affecting dinoflagellate assemblages in recent sediments from trondheimsfjord, Norway. Review of Palaeobotany and Palynology 22, 39–60.

Dale, B., 1996. Dinoflagellate cyst ecology: modeling and geological applications. In: Jansonius, J., McGregor, D.C. (Eds.), Palynology: Principles and Applications, vol. 3. American Association of Stratigraphic Palynologists Foundation, Salt Lake City, pp. 1249–1275.

Dale, B., 2009. Eutrophication signals in the sedimentary record of dinoflagellate cysts in coastal waters. Journal of Sea Research 61, 103–113.

Dale, B., Thorsen, T.A., Fjellså, A., 1999. Dinoflagellate cysts as indicators of cultural eutrophication in the Oslofjord, Norway. Estuarian and Coastal Shelf Science 48, 371–382.

Dale, B., Dale, A.L., Jansen, J.H.F., 2002. Dinoflagellate cysts as environmental indicators in surface sediments from the Congo deep-sea fan and adjacent regions. Palaeogeography, Palaeoclimatology, Palaeoecology 185, 309–338.

de Vernal, A., Henry, M., Matthiessen, J., Mudie, P., Rochon, A., Boessenkool, K.P., Eynaud, F., GrØsfield, K., Guior, J., Hamel, D., Harland, R., Head, M.J., Kunz-Pirrung, M., Levac, E., Loucheur, V., Peyron, O., Pospelova, V., Radi, T., Turon, J.-L., Voronina, E., 2001. Dinoflagellate cyst assemblages as tracers of sea-surface conditions in the northern North Atlantic, Arctic and sub-Arctic seas: the new '$n=677$' database and its application for quantitative palaeoceanographic reconstruction. Journal of Quaternary Science 16, 681–698.

de Vernal, A., Eynaud, F., Henry, M., Hillaire-Marcel, C., Londeix, L., Mangin, S., Matthiessen, J., Marret, F., Radi, T., Rochon, A., Solignaca, S., Turon, J.-L., 2005. Reconstruction of sea-surface conditions at middle to high latitudes of the Northern Hemisphere during the Last Glacial Maximum (LGM) based on dinoflagellate cyst assemblages. Quaternary Science Reviews 24, 897–924.

Ellegaard, M., Clarke, A.L., Ruess, N., Drew, S., Weckström, K., Juggins, S., Anderson, N.J., Conley, D.J., 2006. Multi-proxy evidence of long-term changes in ecosystem structure in a Danish marine estuary, linked to increased nutrient loading. Estuarine, Coastal and Shelf Science 68, 567–578.

Fensome, R.A., Taylor, F.J.R., Norris, G., Sarjeant, W.A.S., Wharton, D.I., Williams, G.L., 1993. A classification of living and fossil dinoflagellates. Micropaleontology (Special Publication) 7, 1–351.

Foreman, M.G.G., Walters, R.A., Henry, R.F., Keller, C.P., Dolling, A.G., 1995. A tidal model for eastern Juan de Fuca Strait and the southern Strait of Georgia. Journal of Geophysical Research 100, 721–740.

González, C., Dupont, L.M., Mertens, K., Wefer, G., 2008. Reconstructing marine productivity of the Cariaco Basin during marine isotope stages 3 and 4 using organic-walled dinoflagellate cysts. Paleoceanography 23, PA3215.

Harland, R., Pudsey, C.J., Howe, J.A., FitzPatrick, M.E.J., 1998. Recent dinoflagellate cysts in a transect from the Falkland trough to the Weddell Sea, Antarctica. Palaeontology 41, 1093–1131.

Harland, R., Nordberg, K., Filipsson, H.L., 2006. Dinoflagellate cysts and hydrographical change in Gullmar Fjord, west coast of Sweden. Science of the Total Environment 355, 204–231.

Head, M.J., 1996. Modern dinoflagellate cysts and their biological affinities. In: Jansonius, J., McGregor, D.C. (Eds.), Palynology: Principles and Applications, vol. 3. American Association of Stratigraphic Palynologists Foundation, Salt Lake City, pp. 1197–1248.

Head, M.J., 2002. *Echinidinium zonneveldiae* sp. nov., a dinoflagellate cyst from the Late Pleistocene of the Baltic Sea, northern Europe. Journal of Micropaleontology 21, 169–173.

Head, M.J., Harland, R., Matthiessen, J., 2001. Cold marine indicators of the late quaternary: the new dinoflagellate cyst genus Islandinium and related morphotypes. Journal of Quaternary Science 16, 621–636.

Hodgins, D.O., 2006. Technical memorandum: assessment of plume trapping and dilution at Clover Point Outfall and Macaulay Point Outfall. Report prepared for the Capital Regional District.

Hodgins, D.O., Tinis, S.W., Taylor, L.A., 1998. Marine sewage outfall assessment for the Capital Regional District, British Columbia, using nested three-dimensional models. Water Science and Technology 38, 301–308.

Holzwarth, U., Esper, O., Zonneveld, K.A.F., 2007. Distribution of organic-walled dinoflagellate cysts in shelf surface sediments of the Benguela upwelling system in relationship to environmental conditions. Marine Micropaleontology 64, 91–119.

Holzwarth, U., Esper, O., Zonneveld, K.A.F., 2010. Organic-walled dinoflagellate cysts as indicators of oceanographic conditions and terrigenous input in the North–West African upwelling region. Review of Paleobotany and Palynology 159 (1–2), 35–55.

Jacobson, D.M., Anderson, D.M., 1986. Thecate heterotrophic dinoflagellates: feeding behaviour and mechanics. Journal of Phycology 22, 249–258.

Jeong, H.J., Kim, S.K., Kim, J.S., Kim, S.T., Yoo, Y.D., Yoon, J.Y., 2001. Growth and grazing rates of the heterotrophic dinoflagellate *Polykrikos kofoidii* on red-tide and toxic dinoflagellates. Journal of Eukaryotic Microbiology 48, 298–308.

Johannessen, S.C., Macdonald, R.W., Paton, D.W., 2003. A sediment and organic carbon budget for the greater Strait of Georgia. Estuarine, Coastal and Shelf Science 56, 845–860.

Kawami, H., van Wezel, R., Koeman, R.P.T., Matsuoka, K., 2009. *Protoperidinium tricingulatum* sp. nov. (Dinophyceae), a new motile form of a round, brown and spiny dinoflagellate cyst. Phycological Research 57, 259–267.

Lavelle, J.W., Massoth, G.J., Crecelius, E.A., 1986. Accumulation rates of recent sediments in Puget Sound, Washington. Marine Geology 72, 59–70.

Lentin, J.K., Williams, G.L., 1993. Fossil dinoflagellates: index to genera and species 1993 edition. American Association of Stratigraphic Palynologists Contribution Series 28. Dallas, Texas.

Lewis, J., Dodge, J.D., Powell, A.J., 1990. Quaternary dinoflagellate cysts from the upwelling system offshore Peru, Hole 696B, ODP Leg 112. In: Suess, E., von Huene, R., et al. (Eds.), Proceeding of the Ocean Drilling Program. Scientific Results 112, pp. 323–327.

Mackas, D.L., Harrison, P.J., 1997. Nitrogenous nutrient sources and sinks in the Juan de Fuca Strait/Strait of Georgia/Puget sound estuarine system: assessing the potential for eutrophication. Estuarine, Coastal and Shelf Science 44, 1–21.

Marret, F., Zonneveld, K.A.F., 2003. Atlas of modern organic-walled dinoflagellate cyst distribution. Review of Palaeobotany and Palynology 125, 1–200.

Marret, F., Scourse, J., Kennedy, H., Ufkes, E., Jansen, J.H.F., 2008. Marine production in the Congo-influenced SE Atlantic over the past 30,000 years: a novel dinoflagellate-cyst based transfer function approach. Marine Micropaleontology 68, 198–222.

Matsuoka, K., 1999. Eutrophication process recorded in dinoflagellate cyst assemblages—a case of Yokohama Port, Tokyo Bay, Japan. The Science of the Total Environment 231, 17–35.

Matsuoka, K., Joyce, L.B., Kotani, Y., Matsuyama, Y., 2003. Modern dinoflagellate cysts in hypertrophic coastal waters of Tokyo Bay, Japan. Journal of Plankton Research 25, 1461–1470.

Matsuoka, K., Kawami, H., Nagai, S., Iwataki, M., Takayama, H., 2009. Re-examination of cyst–motile relationships of *Polykrikos kofoidii* Chatton and *Polykrikos schwartzii* Bütschli (Gymnodiniales, Dinophyceae). Review of Palaeobotany and Palynology 154, 79–90.
McQuoid, M.R., Whiticar, M.J., Calvert, S.E., Pedersen, T.F., 2001. A post-glacial isotope record of primary production and accumulation in the organic sediments of Saanich Inlet ODP Leg 169S. Marine Geology 174, 273–286.
Meyers, P.A., 1994. Preservation of elemental and isotopic source identification of sedimentary organic matter. Chemical Geology 114, 289–302.
Mortlock, R.A., Froelich, P.N., 1989. A simple method for the rapid determination of biogenic opal in pelagic marine sediments. Deep-Sea Research 36, 1415–1426.
Mudie, P.J., Rochon, A., Levac, E., 2002. Palynological records of red tide-producing species in Canada: past trends and implications for the future. Palaeogeography, Palaeoclimatology, Palaeoecology 180, 159–186.
Nelson, D.M., Tréguer, P., Brzezinski, M.A., Leynaert, A., Quéguiner, B., 1995. Production and dissolution of biogenic silica in the ocean: revised global estimates, comparison with regional data and relationship to biogenic sedimentation. Global Biogeochemical Cycles 9, 359–372.
Nixon, S.W., 1995. Coastal marine eutrophication: a definition, social causes and future concerns. Ophelia 41, 199–219.
Pedersen, T.F., Calvert, S.E., 1990. Anoxia vs. productivity: what controls the formation of organic-carbon-rich sediments and sedimentary rocks? AAPG Bulletin 74 454–466.
Pospelova, V., Head, M.J., 2002. *Islandinium brevispinosum* sp. nov. (Dinoflagellata), a new organic-walled dinoflagellate cyst from modern estuarine sediments of New England (USA). Journal of Phycology 38, 593–601.
Pospelova, V., Kim, S.-J., 2010. Dinoflagellate cysts in recent estuarine sediments from aquaculture sites of southern South Korea. Marine Micropaleontology 76, 37–51.
Pospelova, V., Chmura, G.L., Walker, H.A., 2004. Environmental factors influencing the special distribution of dinoflagellate cyst assemblages in shallow lagoons of southern New England (USA). Review of Palaeobotany and Palynology 128, 7–34.
Pospelova, V., Pedersen, T.F., de Vernal, A., 2006. Dinoflagellate cysts as indicators of climatic and oceanographic changes during the past 40 kyr in the Santa Barbara Basin, Southern California. Paleoceanography 21 (PA2101), 1–16.
Pospelova, V., de Vernal, A., Pedersen, T.F., 2008. Distribution of dinoflagellate cysts in surface sediments from the northeastern Pacific Ocean (43–25 °N) in relation to sea-surface temperature, salinity, productivity and coastal upwelling. Marine Micropaleontology 68, 21–48.
Pospelova, V., Chmura, G.L., Boothman, W.S., Latimer, J.S., 2002. Dinoflagellate cyst records and human disturbance in two neighbouring estuaries, New Bedford Harbour and Apponagansett Bay, Massachusetts (USA). The Science of the Total Environment 298, 81–102.
Pospelova, V., Chmura, G.L., Boothman, W.S., Latimer, J.S., 2005. Spatial distribution of modern dinoflagellate cysts in polluted estuarine sediments from Buzzards Bay (Massachusetts, USA) embayments. Marine Ecology Progress Series 292, 23–40.
Radi, T., de Vernal, A., 2004. Dinocyst distribution in surface sediments from the northeastern Pacific margin (40–60 °N) in relation to hydrographic conditions, productivity and upwelling. Review of Palaeobotany and Palynology 128, 169–193.
Radi, T., Pospelova, V., de Vernal, A., Barrie, J.V., 2007. Dinoflagellate cysts as indicators of water quality and productivity in British Columbia estuarine environments. Marine Micropaleontology 62, 269–297.
Ragueneau, O., Treguer, P., Leynaert, A., Anderson, R.F., Brzezinski, M.A., DeMaster, D.J., Dugdale, R.C., Dymond, J., Fisher, G., Francois, R., Heinze, C., Maier-Reimer, E., MartinJezequel, V., Nelson, D.M., Quequiner, B., 2000. A review of the Si cycle in the modern ocean: recent progress and missing gaps in the application of biogenic opal as a paleoproductivity proxy. Global and Planetary Change 26, 317–365.
Reichart, G.-J., Brinkhuis, H., 2003. Late Quaternary Protoperidinium cysts as indicators of paleoproductivity in the northern Arabian Sea. Marine Micropaleontology 49, 303–315.
Rochon, A., de Vernal, A., Turon, J.-L., Matthiessen, J., Head, M.J., 1999. Distribution of Recent dinoflagellate cysts in surface sediments from the North Atlantic Ocean and adjacent seas in relation to sea-surface parameters. American Association of Stratigraphic Palynologists Foundation, Contribution Series 35, Dallas, TX.
Stephens, C., Antonov, J.L., Boyer, T.P., Conkright, M.E., Locarnini, R.A., O'Brien, T.D., Garcia, H.E., 2002. World Ocean Atlas 2001, Volume 1: Temperature. In: Levitus, S. (Ed.), NOAA Atlas NESDIS 49. U.S. Government Printing Office, Wash., D.C., pp. 167.
Stockmarr, J., 1977. Tablets with spores used in absolute pollen analysis. Pollen Spores 13, 615–621.
Stubblefield, W.A., Servos, M., Gersberg, R.M., Riley, C., Simpson, D., Smith, D., Wells, P., 2006. Scientific and technical review. Capital Regional Core Area Liquid Waste Management Plan. Available at 〈www.crd.bc.ca〉.
Taylor, F.G.R., 1987. Ecology of dinoflagellates. In: Taylor, F.G.R. (Ed.), The Biology of Dinoflagellates. Botanical Monograph, 21; 1987, pp. 399–529.
ter Braak, C.J.F., Smilauer, P., 2002. CANOCO reference manual and CanoDraw for windows user's guide: software for Canonical community ordination (version 4.5). Microcomputer Power, Ithaca NY, USA. Available at: 〈www.canoco.com〉.
Thibodeau, B., de Vernal, A., Mucci, A., 2006. Recent eutrophication and consequent hypoxia in the bottom waters of the Lower St. Lawrence Estuary: micropaleontological and geochemical evidence. Marine Geology 231, 37–50.
Thomson, R.E., Mihály, S.F., Kulikov, E.A., 2007. Estuarine versus transient flow regimes in Juan de Fuca Strait. Journal of Geophysical Research 112, 1–25.
Thorsen, T.A., Dale, B., 1997. Dinoflagellate cysts as indicators of pollution and past climate in a Norwegian fjord. Holocene 7, 433–446.
Verado, D.J., Froelich, P.N., McIntyre, A., 1990. Determination of organic carbon and nitrogen in marine sediments using the Carlo Erba NA-1500 Analyzer. Deep-Sea Research 37, 156–165.
Versteegh, G.J.M., Zonneveld, K.A.F., 2002. Use of selective degradation to separate preservation from productivity. Geology 30, 615–618.
Wall, D., Dale, B., 1966. Living fossils in Western Atlantic plankton. Nature 211, 1025–1026.
Wall, D., Dale, B., Lohmann, G.P., Smith, W.K., 1977. The environmental and climatic distribution of dinoflagellate cysts in Modern marine sediments from regions in the North and South Atlantic Oceans and adjacent seas. Marine Micropaleontology 2, 121–200.
Zonneveld, K.A.F., 1997. New species of organic walled dinoflagellate cysts from modern sediments of the Arabian Sea (Indian Ocean). Review of Palaeobotany and Palynology 97, 319–337.
Zonneveld, K.A.F., Versteegh, G.J.M., de Lange, G.J., 1997. Preservation of organic walled dinoflagellate cysts in different oxygen regimes: a 10,000 years natural experiment. Marine Micropaleontology 29, 393–405.
Zonneveld, K.A.F., Hoek, R.P., Brinkhuis, H., Willems, H., 2001. Geographical distributions of organic-walled dinoflagellate cysts in surficial sediments of the Benguela upwelling region and their relationship to upper ocean conditions. Progress in Oceanography 48, 25–72.
Zonneveld, K.A.F., Bockelmann, F., Holzwarth, U., 2007. Selective preservation of organic-walled dinoflagellate cysts as a tool to quantify past net primary productivity and bottom water oxygen concentrations. Marine Geology 237, 109–126.
Zonneveld, K.A.F., Versteegh, G., Kodrans-Nsiah, M., 2008. Preservation and organic chemistry of Late Cenozoic organic-walled dinoflagellate cysts: a review. Marine Micropaleontology 68, 179–197.
Zonneveld, K.A.F., Chen, L., Möbius, L., Mahmoud, M.S., 2009. Environmental significance of dinoflagellate cysts from the proximal part of the Po-river discharge plume (off southern Italy, Eastern Mediterranean). Journal of Sea Research 62 (4), 189–213.